THE JOURNAL OF BIOLOGICAL CHEMISTRY VOL. 281, NO. 11, pp. 7666–7683, March 17, 2006

Four and a Half LIM Protein 1 Binds Myosin-binding Protein C and Regulates Myosin Filament Formation and Sarcomere Assembly*

Received for publication, November 23, 2005 Published, JBC Papers in Press, January 9, 2006, DOI 10.1074/jbc.M512552200

Meagan J. McGrath[‡], Denny L. Cottle[‡], Mai-Anh Nguyen[§], Jennifer M. Dyson[‡], Imogen D. Coghill[‡], Paul A. Robinson[‡], Melissa Holdsworth[‡], Belinda S. Cowling[‡], Edna C. Hardeman[§], Christina A. Mitchell[‡1], and Susan Brown[‡]

From the [‡]Department of Biochemistry and Molecular Biology, Monash University, Victoria 3800 and [§]Muscle Development Unit, Children's Medical Research Institute, Westmead, New South Wales 2145, Australia

Four and a half LIM protein 1 (FHL1/SLIM1) is highly expressed in skeletal and cardiac muscle; however, the function of FHL1 remains unknown. Yeast two-hybrid screening identified slow type skeletal myosin-binding protein C as an FHL1 binding partner. Myosin-binding protein C is the major myosin-associated protein in striated muscle that enhances the lateral association and stabilization of myosin thick filaments and regulates actomyosin interactions. The interaction between FHL1 and myosin-binding protein C was confirmed using co-immunoprecipitation of recombinant and endogenous proteins. Recombinant FHL2 and FHL3 also bound myosin-binding protein C. FHL1 impaired co-sedimentation of myosin-binding protein C with reconstituted myosin filaments, suggesting FHL1 may compete with myosin for binding to myosin-binding protein C. In intact skeletal muscle and isolated myofibrils, FHL1 localized to the I-band, M-line, and sarcolemma, co-localizing with myosin-binding protein C at the sarcolemma in intact skeletal muscle. Furthermore, in isolated myofibrils FHL1 staining at the M-line appeared to extend partially into the C-zone of the A-band, where it co-localized with myosin-binding protein C. Overexpression of FHL1 in differentiating C2C12 cells induced "sac-like" myotube formation (myosac), associated with impaired Z-line and myosin thick filament assembly. This phenotype was rescued by co-expression of myosin-binding protein C. FHL1 knockdown using RNAi resulted in impaired myosin thick filament formation associated with reduced incorporation of myosin-binding protein C into the sarcomere. This study identified FHL1 as a novel regulator of myosin-binding protein C activity and indicates a role for FHL1 in sarcomere assembly.

In striated muscle LIM proteins play critical roles in scaffolding sarcomeric and signaling proteins (1–8). LIM proteins are defined by the presence of one or more LIM domains, a cysteine-rich double zinc finger protein-binding motif denoted by the sequence (CX_2-$CX_{17-19}HX_2C)X_2(CX_2CX_{16-20}CX_2$(H/D/C)) (9). The four and a half LIM (FHL)[2] proteins are a family of LIM-only proteins, characterized by four complete LIM domains, preceded by an N-terminal half LIM domain (10). To date five family members FHL1–4 and activator of CREM in testis (ACT) have been identified. FHL1, FHL2, and FHL3 are all expressed in striated muscle (11). FHL2 and FHL3 are well characterized, and multiple protein binding partners have been identified. In the nucleus FHL2 and FHL3 bind and regulate the activity of multiple transcription factors, including the androgen receptor, AP-1 (activator protein-1), CREB (cyclic AMP-response element-binding protein), PLZF (promyelocytic leukemia zinc finger protein), extracellular signal-regulated kinase 2 (ERK2), β-catenin, and FOXO1(Forkhead box class O protein 1) (10, 12–18). FHL2 and FHL3 also localize to the cytoskeleton where they bind integrin receptors (19, 20). We have reported previously that in myoblasts FHL3 binds skeletal α-actin and inhibits α-actinin-mediated actin cross-linking, suggesting that FHL proteins may also play an important role in regulating cytoskeletal dynamics (21).

FHL1 is the least characterized of the FHL proteins and is the focus of this study. To date, the role of FHL1 in striated muscle is unknown, and binding partners have not been characterized. In this study, to investigate the function of FHL1 in skeletal muscle, yeast two-hybrid screening of a human skeletal muscle library was undertaken and identified myosin-binding protein C (MyBP-C) as an FHL1-binding partner. MyBP-C constitutes ~1–2% of the total myofibrillar protein and is proposed to function as one of the major myosin-thick filament regulatory proteins (22). Three isoforms of MyBP-C, each encoded by separate genes, have been identified as follows: slow and fast type skeletal muscle and cardiac MyBP-C (23–25). The domain organization is conserved throughout all MyBP-C isoforms, comprising seven immunoglobulin-C2 domains (Ig-C2) (C1–C5, C8, and C10) and three fibronectin type III motifs (C6, C7, and C9). In addition, cardiac MyBP-C also contains a unique N-terminal Ig-C2 domain (C0).

In mature striated muscle MyBP-C localizes to the cross-bridge (C-zone) of the A-band, where multiple domains bind myosin and titin (26). In all MyBP-C isoforms, the primary myosin-binding site resides in the C-terminal IgC2 domain C10 (27–29). More specifically, this C10 domain binds the light meromyosin (LMM) or rod region of myosin, which forms the backbone of the thick filament (27, 30). In addition, the N-terminal Ig-C2 domains C1–C2 of MyBP-C bind subfragment 2 (S2) of myosin, which includes the junction between the myosin head and thick filament backbone (31, 32). The N-and C-terminal binding of MyBP-C to myosin is proposed to form a dynamic, interconnected network with myosin to tether and regulate myosin flexibility and hence interaction with actin.

* The costs of publication of this article were defrayed in part by the payment of page charges. This article must therefore be hereby marked "*advertisement*" in accordance with 18 U.S.C. Section 1734 solely to indicate this fact.

[1] To whom correspondence should be addressed: Dept. of Biochemistry and Molecular Biology, Monash University, Wellington Rd., Clayton, Victoria 3800, Australia. Tel.: 61-3-9905-1245; Fax: 61-3-9905-3790; E-mail: christina.mitchell@med.monash.edu.au.

[2] The abbreviations used are: FHL, four and a half LIM protein; cMyBP-C, cardiac MyBP-C, myosin-binding protein C; MyHC, myosin heavy chain; Ig-C2, immunoglobulin-C2 domain; stMyBP-C, slow type MyBP-C; Y2H, yeast two-hybrid; RNAi, RNA interference; HA, hemagglutinin; siRNA, small interfering RNA; FITC, fluorescein isothiocyanate; GST, glutathione *S*-transferase; PBS, phosphate-buffered saline; LMM, light meromyosin.

TABLE 1
Oligonucleotides used to generate FHL1 and cardiac MyBP-C constructs

Name of construct	5′-Oligonucleotide	3′-Oligonucleotide	Polypeptide expressed
Yeast two-hybrid			
pGBKT7-FHL1	5′-ggaattcatggcggagaagtttgactgc-3′	5′-ggaattcttacagctttttggcacagtc-3′	FHL1 full-length (amino acids 1–280)
pGBKT7-FHL1 (1/2 LIM 1 + 2)	5′-ggaattcatggcggagaagtttgactgc-3′	5′-ggaattcttacttggtctcatggcaagt-3′	FHL1 LIM domains 1/2, 1 and 2) (amino acids 1–157)
MyBP-C constructs			
FLAG-cMyBP-C	5′-gacgcgtgaattcatgcctgagccggggaagaag-3′	5′-cacgcgtgaattctatcactgaggcactcgcacctc-3′	cMyBP-C full-length (amino acids 1–1274)
FLAG-cMyBP-C (Δ FHL1/BD)	5′-gacgcgtgaattcatgcctgagccggggaagaag-3′	5′-cacgcgtgaattcatcatctaatctccagagtcaacac-3′	cMyBP-C minus region identified by FHL1 in yeast two-hybrid (amino acids 1–1225)
GST-cMyBP-C (C6–C10)	5′-ggaattctaatgccagacgcacctgcggccccc-3′	5′-cacgcgtgaattctatcactgaggcactcgcacctc-3′	cMyBP-C domains C6–C10 (amino acids 772–1274)

The role of MyBP-C in striated muscle is contentious; however, MyBP-C may be required for the formation and stabilization of normal myosin thick filaments and for the regulation of myosin cross-bridge kinetics (22, 25). *In vitro* MyBP-C is required for the efficient formation of long, uniform, and compact thick filaments (27, 33). The C10 myosin binding domain is essential for the ability of MyBP-C to polymerize myosin (34–36).

MyBP-C is also predicted to play an important role in sarcomere formation during myofibrillogenesis. Expression of MyBP-C lacking the C10 domain, in skeletal myotubes and cardiomyocytes, potently inhibits sarcomere formation (37, 38). Cardiac MyBP-C(+) is a recently identified splice variant, which contains a 10-amino acid insert within the C-terminal domain C9 (38). Cardiac MyBP-C(+) exhibits reduced binding affinity for myosin and titin *in vitro* and disrupts sarcomere formation when expressed in cardiomyocytes. Collectively, these studies highlight the importance of the C10 myosin-binding domain to MyBP-C activity. Most interestingly, mutations in cardiac MyBP-C, which commonly result in loss of the C-terminal titin and/or myosin binding domains, are the second leading cause of familial hypertrophic cardiomyopathy (24, 39, 40).

In this study we have demonstrated a functional interaction between MyBP-C and FHL1. FHL1 localized predominantly to the I-band of mature skeletal muscle sections and isolated myofibrils. Furthermore, a pool of FHL1 was detected at the M-line that extended into the C-zone of the A-band, co-localizing with MyBP-C. In an *in vitro* assay FHL1 impaired the co-sedimentation of MyBP-C with myosin filaments, suggesting FHL1 and myosin compete for binding to domain C10 of MyBP-C. Overexpression of FHL1 and RNAi-mediated knockdown of FHL1 in differentiating C2C12 cells indicate FHL1 is a novel regulator of MyBP-C activity and thereby sarcomeric assembly.

EXPERIMENTAL PROCEDURES

Materials—pEFBOS was provided by Dr. T. Wilson (WEHI, Australia). Human skeletal muscle cDNA library and pEGFP-C2 vector were from Clontech. The human cMyBP-C cDNA was from Dr. L. Carrier (Institute of Experimental and Clinical Pharmacology, Eppendorf University Hospital, Hamburg, Germany). Cell lines were from American Type Culture Collection. The following antibodies were used: HA (Sigma); FLAG, α-actinin, and vinculin (Sigma); myosin heavy chain (Biocytex Biotechnology); and β-tubulin (Zymed Laboratories Inc.). The rabbit polyclonal FHL1 antibody is directed against a unique amino acid sequence located in the fourth LIM domain of human FHL1 as described previously (41–43). The rabbit polyclonal FHL3 antibody was also generated previously (21). The FHL2 antibody was generated by immunizing New Zealand White rabbits with a synthetic peptide that contained the first six N-terminal amino acids (MTERFD) and the last six C-terminal amino acids (DCGKDI) conjugated to diphtheria toxin by a central cysteine residue. This antibody only recognizes FHL2 and not FHL1 or FHL3 as shown by immunoblot analysis of recombinant proteins (data not shown). The monoclonal slow type (ALD66) MyBP-C antibody (44) and the myosin heavy chain (MF20, sarcomeric) antibody, were from the Developmental Studies Hybridoma Bank developed under the auspices of the NICHD, National Institutes of Health, and maintained by the Department of Biological Sciences, University of Iowa, Iowa City. Prior to use the slow type MyBP-C antibody was concentrated using a Centriplus centrifugal filter device (YM-50) (Millipore) according to the manufacturer's instructions.

Glutathione-Sepharose and the GST antibody were from Amersham Biosciences. Talon resin was from BD Biosciences, and the anti-polyhistidine antibody was from Sigma. Lipofectamine and Lipofectamine 2000 were from Invitrogen. Unless otherwise stated, all other reagents were from Sigma.

Yeast Two-hybrid—The Matchmaker 3 GAL4 Y2H system (Clontech) was used. The cDNA sequence encoding the N-terminal half LIM domain and LIM domains 1 and 2 of FHL1 (1/2 1 + 2) was cloned into the EcoRI site of pGBKT7 in-frame with the GAL4 DNA-binding domain ("bait") (Table 1 and Fig. 1*A*). AH109 yeast expressing the pGBKT7-FHL1 bait were mated with Y187 yeast transformed with a human skeletal muscle cDNA library, fused to the GAL4 activation domain. Transformants were screened as per the manufacturer's instructions, and plasmids from positive clones were extracted and sequenced. A bait compromising the N-terminal two and a half LIM domains (1/2 1 + 2) of FHL3 (amino acids 1–161) and the C-terminal LIM domains 3 and 4 from FHL2 (amino acids 156–280) were also used to screen a human skeletal muscle library.

In Vitro GST Pull-down—Domains C6–C10 of cMyBP-C (amino acids 772–1274) (GenBank™ accession number Q14896) (Table 1) were cloned into the EcoRI site of the pGEX-1λT vector in-frame with the upstream GST tag. Expression of recombinant GST or GST-cMyBP-C (C6–C10) was induced in *Escherichia coli*, and protein was extracted overnight, as described previously, and incubated with glutathione-Sepharose for 6 h at 4 °C (21). The pGBKT7-FHL1 construct was linearized (SalI), and protein was translated in the presence of [^{35}S]methionine using the TNT wheat germ extract system (Promega). 100 μl of ^{35}S-FHL1 was incubated with GST-conjugated Sepharose overnight at 4 °C and then washed extensively with Tris-buffered saline (20 mM Tris, 150 mM NaCl, pH 7.4) containing 1% Triton X-100. Bound ^{35}S-FHL1 was eluted with SDS-PAGE reducing buffer. Unbound and bound samples were run on SDS-PAGE, Western-transferred, and exposed to Biomax emulsion film (Eastman Kodak). Bound samples were also immunoblotted with anti-GST (1:1000) to confirm conjugation of GST-tagged proteins to Sepharose.

Generation of FHL and cMyBP-C Constructs—β-Galactosidase, FHL1, FHL2, and FHL3 cDNA were cloned previously into the XbaI site of the pCGN vector (21, 42). The full-length cMyBP-C cDNA was

cloned into the MluI site of the pEFBOS-FLAG vector to generate a fusion protein containing an N-terminal FLAG tag. A C-terminal truncation mutant of cMyBP-C, cMyBP-C(ΔFHL1/BD) (amino acids 1–1225), was also cloned into the MluI site of the pEFBOS-FLAG vector (Table 1).

Growth of Sol8, C2C12, and COS-1 Cells—The Sol8 and C2C12 mouse skeletal myoblast cell lines were grown at low confluence in Dulbecco's modified Eagle's medium containing 20% fetal calf serum, 2 mM L-glutamine, 100 units/ml penicillin, and 0.1% streptomycin. To induce differentiation, cells were grown to confluence and switched to media containing Dulbecco's modified Eagle's medium, 5% horse serum, 2 mM L-glutamine, 100 units/ml penicillin and 0.1% streptomycin for 96–144 h. COS-1 cells were maintained in Dulbecco's modified Eagle's medium supplemented with 10% fetal calf serum, 2 mM L-glutamine, 100 units/ml penicillin, and 0.1% streptomycin.

Co-immunoprecipitation of FHL and MyBP-C from COS-1 Cells—COS-1 cells maintained in 100-mm dishes were co-transfected with 5 μg of DNA (per construct) using electroporation at 200 V and 975 microfarads. 48 h post-transfection cells were washed in phosphate-buffered saline and lysed in Tris saline containing 1% Triton X-100 and protease inhibitors for 2 h at 4 °C. Lysates (1 ml) were centrifuged at 15,400 × *g* for 5 min and pre-cleared with 60 μl of protein A-Sepharose (50% slurry) for 1 h at 4 °C. Pre-cleared lysates were immunoprecipitated with 10 μg of monoclonal FLAG, HA, or nonimmune control antibodies together with 60 μl of protein A-Sepharose overnight at 4 °C. The Sepharose was washed thoroughly with lysis buffer, and precipitated protein was eluted with SDS-PAGE reducing buffer. Immunoprecipitates and cell lysates were separated by SDS-PAGE and immunoblotted with FLAG or HA antibodies (1:5000).

Co-immunoprecipitation of Endogenous FHL1 and stMyBP-C—Sol8 myotube Triton-soluble lysates were prepared and pre-cleared with protein A-Sepharose as above. 50 μg of anti-stMyBP-C, anti-FHL1, or nonimmune control antibodies was incubated with 60 μl of protein A-Sepharose for 1 h at 4 °C. The antibody-conjugated Sepharose was collected by centrifugation at 1,500 × *g* for 30 s at 4 °C and incubated with cell lysates overnight at 4 °C. Sepharose was washed as described above, separated by SDS-PAGE, and immunoblotted with a mouse stMyBP-C antibody or the FHL1 antibody.

In Vitro Co-sedimentation Binding Assay—Domains C6–C10 of cMyBP-C (amino acids 772–1274) were excised from the pGEX-1λT vector (described above) using EcoRI and cloned into the pTrcHisA vector (Invitrogen) in-frame with the upstream polyhistidine tag. Similarly, full-length FHL1 was excised from the pEGFP-C2 vector using EcoRI and cloned into the pGEX-5X-1 vector in-frame with the upstream GST tag. Expression of recombinant GST, GST-FHL1, or His-cMyBP-C (C6–C10) was induced in *E. coli* at 23 °C for 2 h following the addition of 0.1 mM isopropyl 1-thio-β-D-galactopyranoside. Recombinant protein was extracted from bacteria, as described previously (21), purified using glutathione-Sepharose (GST) or talon resin (His), and concentrated using a Centriplus centrifugal filter device (Millipore) (YM-50 for GST-FHL1 or His-cMyBP-C (C6–C10) and YM-30 for GST alone). An aliquot of purified recombinant protein was separated by SDS-PAGE, stained with Coomassie Brilliant Blue, and the protein concentration determined using densitometry.

Co-sedimentation assays were modified from Refs. 28 and 38. Synthetic myosin filaments were generated by incubating 0.5 μM of myosin purified from rabbit skeletal muscle (Sigma) in binding buffer (20 mM imidazole, 10 mM reduced glutathione, 0.1 M KCl, pH 7.0, 1 mM dithiothreitol) for 1 h and then rocking at 4 °C. To a final volume of 150 μl, 0.2 μM His-cMyBP-C (C6–C10) and 0.5 μM of either GST alone or GST-FHL1 were added to myosin filaments and incubated overnight with rocking at 4 °C. In control studies, binding buffer was used in lieu of recombinant protein. Myosin filaments were recovered by centrifugation at 106,000 × *g* (50,000 rpm TLA 100.3 rotor, Beckman) for 30 min at 4 °C, followed by removal of the supernatant and reconstitution of filaments (pellet) in 150 μl of SDS-PAGE reducing buffer. 30 μl of pellet fractions were separated by SDS-PAGE and immunoblotted with MyHC (MF20, 1:100), GST (1:1000), or polyhistidine (1:3000) antibodies. In control studies to detect MyBP-C not bound to myosin filaments, 30 μl of the supernatant fraction was also immunoblotted with a polyhistidine antibody.

Tissue Sections—Frozen longitudinal and transverse sections of mouse soleus muscle were prepared as described previously (21). Sections were stained with the FHL1 antibody or preimmune serum, followed by FITC-conjugated anti-rabbit IgG secondary antibody (1:400). Sections were also co-stained with monoclonal antibodies against α-actinin (1:600), vinculin (1:600), MyHC (MF20 1:200), or slow type MyBP-C (0.1 μg/ml) followed by Alexa-594-conjugated anti-mouse IgG secondary antibody (1:600). Sections were viewed using laser scanning confocal microscopy on a Leica TCS NT system (Monash microimaging, Monash University, Australia).

Isolation of Single Myofibrils—The protocol for isolating single myofibrils from murine skeletal muscle was modified from Ref. 45. Mice were killed humanely following the National Health and Medical Research Council guidelines, Monash University animal ethics number BAM/2000/17. Hind legs were removed, skinned, attached to a Perspex stick at resting length, and incubated in rigor buffer (75 mM KCl, 10 mM Tris, 2 mM $MgCl_2$, 2 mM EGTA, 0.5% Triton X-100, protease inhibitor tablet (Roche Applied Science), pH 6.8) overnight at 4 °C. Skeletal muscle was dissected from the bone and minced in 5 volumes (v/w) of ice-cold rigor buffer (minus Triton X-100). To the extract myofibrils samples were homogenized on ice for two intervals of 30 s, and the myofibrils were collected by centrifugation at 1,500 × *g* for 10 min at 4 °C, washed twice with cold rigor buffer (minus Triton X-100), resuspended in rigor buffer (minus Triton X-100), glycerol (1:1), and stored at −20 °C. For immunohistochemistry 100 μl of myofibrils were aliquoted onto Superfrost slides and allowed to adhere for 10 min, fixed with 4% paraformaldehyde for 15 min, washed three times with PBS, and then blocked with PBS containing 10% horse serum and 1% bovine serum albumin for 10 min. Myofibrils were stained with the FHL1 antibody, followed by FITC-conjugated anti-rabbit IgG secondary (1:400). Myofibrils were also co-stained with monoclonal antibodies specific for either α-actinin (1:800), vinculin (1:600), MyHC (MF20 1:200), or slow type MyBP-C (0.1 μg/ml), followed by Alexa-594-conjugated anti-mouse IgG secondary antibody (1:600). For comparison purposes myofibrils were also co-stained with antibodies specific for slow type MyBP-C and either FHL2 or FHL3. All antibodies were diluted in PBS containing 1% bovine serum albumin and incubated for 1 h at room temperature. Coverslips were mounted onto samples using Mowiol mounting media (Calbiochem). Myofibrils were viewed using a Fluoview 1000 laser scanning confocal microscope, and three-dimensional blind deconvolution (10 iterations) was performed using the analySIS® (Olympus) program at Monash MicroImaging, Monash University, Australia. Deconvolution images represent maximum intensity stacks (projections) of optical sections.

Stable Overexpression of HA-βgal Control or HA-FHL1 in C2C12 Cells—pTrio12R-HGN derived from pCGN contains the following: a HA tag and multicloning site from pCGN, followed by an internal ribosome re-entry sequence, a GST tag and MluI cloning site, a second internal ribosome re-entry sequence followed by the neomycin resist-

ance gene (from pFBERV) and contains a mammalian centrimeric origin of replication and matrix attachment region (ORS12) to allow autonomous replication. β-Galactosidase and FHL1 were cloned into the XbaI site of pTrio12R-HGN downstream of the HA tag. The pTrio12R-HGN− constructs were transfected into C2C12 myoblasts using Lipofectamine and stably transfected cells selected in G418-sulfate (1.5 mg/ml) for 3 weeks.

Immunofluorescence of C2C12 Cells—C2C12 myoblasts were plated onto fibronectin-coated coverslips at a density of $1.0 \times 10^4/cm^2$, transiently transfected, and induced to differentiate for 96–144 h into myotubes, fixed, and permeabilized as described previously (42). HA- or FLAG-tagged protein was detected using monoclonal anti-HA (1:1000) or anti-FLAG (1:2000) followed by FITC-conjugated anti-mouse IgG secondary (1:400). Myotubes were also stained with α-actinin (1:600) or MyHC (MF20, 0.1 μg/ml) followed by anti-mouse Alexa-594 secondary antibody (1:600). To detect nuclei, cells were pretreated with 200 μg/ml RNase A for 1 h before staining with 2 μg/ml propidium iodide for 5 min.

RNAi—Two DNA oligonucleotides (Geneworks) specific for murine FHL1 (GenBank™ accession number NM_010211), identified using the "siRNA target finder" at the website (www.ambion.com/techlib/misc/siRNA_finder.html), were used as a template for synthesizing siRNA. Double-stranded siRNA was synthesized from DNA oligonucleotides using the *Silencer* siRNA construction kit (Ambion) according to manufacturer's instructions. For transfection C2C12 myoblasts were plated onto fibronectin (5 μg/ml)-coated coverslips at a density of $1.0 \times 10^4/cm^2$ in a 6-well dish and grown overnight in growth media lacking antibiotics (42). Cells were transiently transfected with 25 nM siRNA using 4 μl of Lipofectamine 2000 (Invitrogen) for 4 h, after which growth media were replaced. 48 h post-transfection cells were either lysed for Western blot analysis or induced to differentiate for immunofluorescence studies. For immunofluorescence studies, cells were treated as described above and stained with either the MyHC (MF20, 0.1 μg/ml) or slow type MyBP-C (0.1 μg/ml) antibodies, followed by anti-mouse FITC-conjugated secondary antibody (1:400). In control studies, to confirm down-regulation of FHL1 expression, C2C12 myoblasts were transfected with FHL1 or scrambled siRNA previously labeled with Cy5 using an siRNA labeling kit (Ambion) and 48 h post-transfection were fixed and stained with an FHL1 antibody.

RESULTS

Identification of MyBP-C as a FHL1 Binding Partner—To identify FHL1-binding proteins, yeast two-hybrid (Y2H) screening of a human skeletal muscle library was performed using a bait comprising the N-terminal two and a half LIM domains of human FHL1 (pGBKT7-FHL1 (LIM 1/2 1 + 2)) (amino acids 1–157) (Fig. 1*A*). On two independent screenings, the C-terminal 50 amino acids (1073–1123) of the C10 domain of slow type skeletal muscle MyBP-C (stMyBP-C), including the stop codon and variable regions of 3′-untranslated region, were isolated (Fig. 1*B*, "*prey*"). Control experiments, to exclude autonomous activation of yeast reporter genes by either the FHL1 bait or stMyBP-C clones, confirmed a *bona fide* protein interaction (data not shown). Three isoforms of MyBP-C have been identified (23, 24) as follows: slow type (st) and fast type (ft) skeletal muscle and cardiac (c) MyBP-C. All three isoforms demonstrate a similar domain structure comprising seven Ig-C2 domains (C1–C5, C8, and C10) and three fibronectin type III motifs (C6, C7, and C9) (Fig. 1*B*). In addition the cardiac isoform also contains a unique N-terminal Ig-C2 domain (C0). The C10 domain that bound FHL1 in Y2H is highly homologous in all three MyBP-C isoforms and also binds the rod (LMM) region of myosin (Fig. 1, *B* and *C*) (22, 28, 29). Therefore, FHL1 may also bind all three MyBP-C isoforms.

FHL1 Binds MyBP-C in Vitro and in Vivo—To demonstrate a direct protein interaction between FHL1 and MyBP-C, *in vitro* protein binding studies were performed using bacterially expressed GST fused to domains C6–C10 of cardiac MyBP-C. Sepharose-conjugated GST-cMyBP-C(C6–C10) or GST alone was incubated with *in vitro* translated ^{35}S-FHL1, and unbound and bound fractions were analyzed by SDS-PAGE and autoradiography. ^{35}S-FHL1 bound to GST-cMyBP-C(C6–C10) but not GST alone, confirming a direct protein interaction (Fig. 2*A*, *upper panel*). In control studies, GST immunoblot analysis confirmed GST and GST-cMyBP-C(C6–C10) were conjugated to the glutathione-Sepharose, with some proteolysis of cMyBP-C (C6–C10) detected (Fig. 2*A*, *lower panel*).

To demonstrate these proteins interact in intact cells, COS-1 cells were co-transfected with full-length hemagglutinin (HA)-tagged FHL1 and FLAG-tagged full-length cardiac MyBP-C. Triton-soluble cell lysates were immunoprecipitated and immunoblotted with antibodies against both tags. FLAG-cMyBP-C was detected in anti-HA, but not nonimmune immunoprecipitates (Fig. 2*B-a*, *upper left panel*). Immunoprecipitation of HA-FHL1 was confirmed by immunoblotting with anti-HA (Fig. 2*B-a*, *upper right panel*). In the reciprocal experiment, HA-FHL1 was co-immunoprecipitated with FLAG but not nonimmune antibodies (Fig. 2*B*, *b*, *upper left panel*). Expression of recombinant proteins was confirmed by immunoblotting lysates with HA and FLAG antibodies (Fig. 2*B*, *a* and *b*, *lower left panels*).

To investigate whether endogenous FHL1 and MyBP-C co-immunoprecipitate, we used a previously characterized FHL1 antibody, directed against a unique amino acid sequence located in the fourth LIM domain of human FHL1 (41–43). This sequence is not found in the alternatively spliced FHL1 isoforms KyoT2 and SLIMMER nor in FHL2 or FHL3 sequences. To confirm specificity of the FHL1, antibody lysates from COS-1 cells expressing either HA-FHL1, HA-FHL2, or HA-FHL3 were immunoblotted with the FHL1 antibody, and only HA-FHL1 was immunoreactive (Fig. 2*C*, *upper panel*). Immunoblotting of the same lysates with HA antibodies confirmed equivalent expression of the recombinant HA-tagged FHL proteins (Fig. 2*C*, *lower panel*). Triton-soluble lysates prepared from Sol8 skeletal myotubes immunoprecipitated with the FHL1 antibody and immunoblotted with an antibody to slow type skeletal MyBP-C demonstrated a 140-kDa polypeptide consistent with the molecular weight of slow type MyBP-C (Fig. 2*D*, *upper panel*). In contrast, slow type MyBP-C was not detected in nonimmune immunoprecipitates. Immunoprecipitation of FHL1 was confirmed by immunoblotting with the FHL1 antibody (Fig. 2*D*, *lower panel*). These studies demonstrate that FHL1 complexes with both cardiac MyBP-C (*in vitro* binding and recombinant co-immunoprecipitation) and slow type skeletal MyBP-C (Y2H screen and endogenous protein co-immunoprecipitation).

FHL1, FHL2, and FHL3 Bind the C Terminus of MyBP-C—The FHL family members FHL2 and FHL3 are expressed in cardiac and skeletal muscle, respectively (11). Yeast two-hybrid screens of a human skeletal muscle library using FHL2 as a bait isolated stMyBP-C (last 19 amino acids of domain C8, all of domain C9 and the C10 domain, excluding the last 20 amino acids (amino acids 895–1104)) (Fig. 3*A*). FHL3 bait screening also isolated stMyBP-C (last 28 amino acids of the C9 domain and all of domain C10 (amino acids 1008–1123)) (Fig. 3*A*).

To demonstrate an interaction between cardiac MyBP-C and either FHL2 or FHL3, COS-1 cells were co-transfected with FLAG-cardiac MyBP-C (FLAG-cMyBP-C) together with either HA-FHL2 or HA-FHL3, and Triton-soluble lysates were immunoprecipitated with

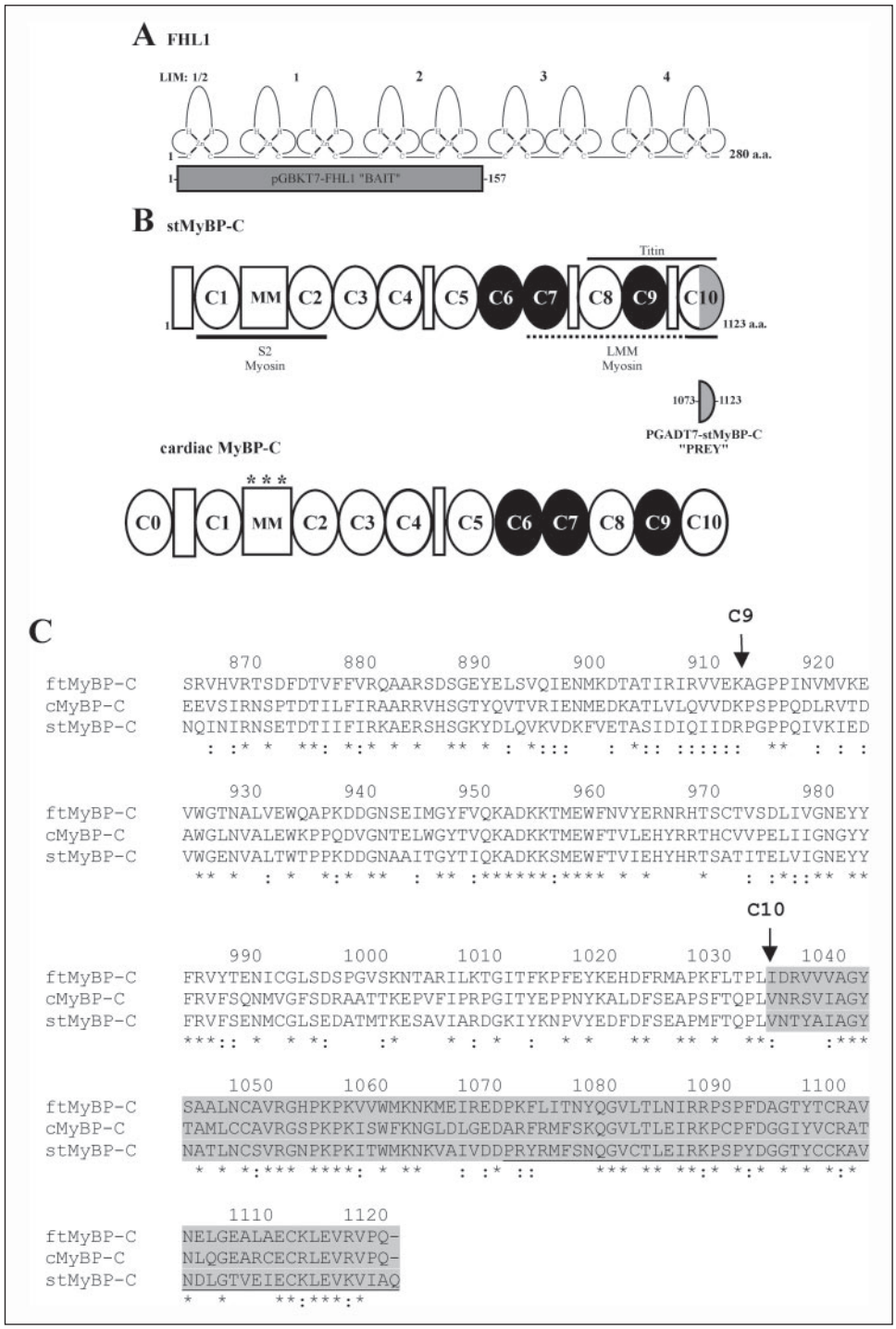

FIGURE 1. **FHL1 binds the C10 domain of skeletal slow type MyBP-C in yeast two-hybrid screening.** *A,* LIM domain structure of FHL1 indicating the N-terminal bait used to screen the skeletal muscle library. *B,* domain structure of slow type (*st*) MyBP-C, indicating the IgC2 domains (*white oval*), fibronectin type III motifs (*black oval*), and the MyBP-C motif (*MM*), with domains mediating binding to myosin and titin indicated (*solid lines*). Domain C10 binds the rod region (*LMM*) of myosin with binding increased by the addition of domains C7–C9 (*broken line*). The clones binding FHL1 in Y2H screening encoded the *shaded* C-terminal half of C10 (pGADT7-stMyBP-C "prey"). The cardiac MyBP-C isoform contains a unique N-terminal Ig-C2 domain (C0), an additional 9 residues, and 3 phosphorylation sites within the MyBP-C motif (asterisk) and a 28-amino acid (*a.a.*) insert within domain C5. *C,* optimized alignment of C-terminal sequences from human skeletal fast type MyBP-C (*ftMyBP-C*) (GenBank™ accession number Q14324), slow type MyBP-C (*stMyBP-C*) (GenBank™ accession number Q00872)m and cardiac MyBP-C (cMyBP-C) (GenBank™ accession number Q14896) isoforms. The multiple sequence alignment was performed using ClustalW (fast) (91). The amino acid sequence is numbered in accordance with the stMyBP-C sequence. ↓ denotes the first amino acid of each domain; an *asterisk* represents identical amino acids, and a *colon* represents conservative substitutions in all three sequences. The C10 domain is shaded *gray*. The stMyBP-C sequence (amino acids 1073–1123 underlined) represents the region identified by FHL1 in a yeast two-hybrid screen.

HA or nonimmune antibodies and immunoblotted with anti-FLAG (Fig. 3*B*). In HA-FHL2 co-transfected cells, FLAG-cMyBP-C was detected in HA but not nonimmune immunoprecipitates (Fig. 3*B*, *a*, *upper left panel*). Similarly in HA-FHL3 co-transfected cells, FLAG-cMyBP-C was co-immunoprecipitated with HA but not nonimmune antibodies (Fig. 3*B*, *b*, *upper left panel*). Immunoprecipitation of either HA-FHL2 or HA-FHL3 was confirmed by immunoblotting with anti-HA (Fig. 3*B, a* and *b*, *upper right panels*). These studies indicate that cardiac MyBP-C is a common binding partner for FHL1, FHL2, and FHL3.

We isolated the C10 domain of MyBP-C as a FHL1 binding partner. Most interestingly, the MyBP-C C10 domain is also the primary myosin-binding site (28, 29). To confirm FHL1 binds to the C10 domain (amino acids 1073–1123) of MyBP-C, a FLAG-tagged cardiac MyBP-C mutant, which lacks the putative FHL1-binding site in the C10 domain (FLAG-cMyBP-C(ΔFHL1/BD)) (Fig. 3*C, schematic*), was co-transfected with FHL1, FHL2, or FHL3 in COS-1 cells. FLAG-cMyBP-C(ΔFHL1/BD) co-immunoprecipitated with HA-FHL2 but not HA-FHL1 or HA-FHL3 (Fig. 3*C, top immunoblot*). Immunoprecipitation of FHL proteins was confirmed by immunoblotting with anti-HA (Fig. 3*C, middle*). Expression of FLAG-cMyBP-C(ΔFHL1/BD) was confirmed by immunoblotting lysates with anti-FLAG (Fig. 3*C, bottom*). Although we cannot exclude the possibility that recombinant FLAG-cMyBP-C(ΔFHL1/BD) misfolds, correct folding is suggested by its abil-

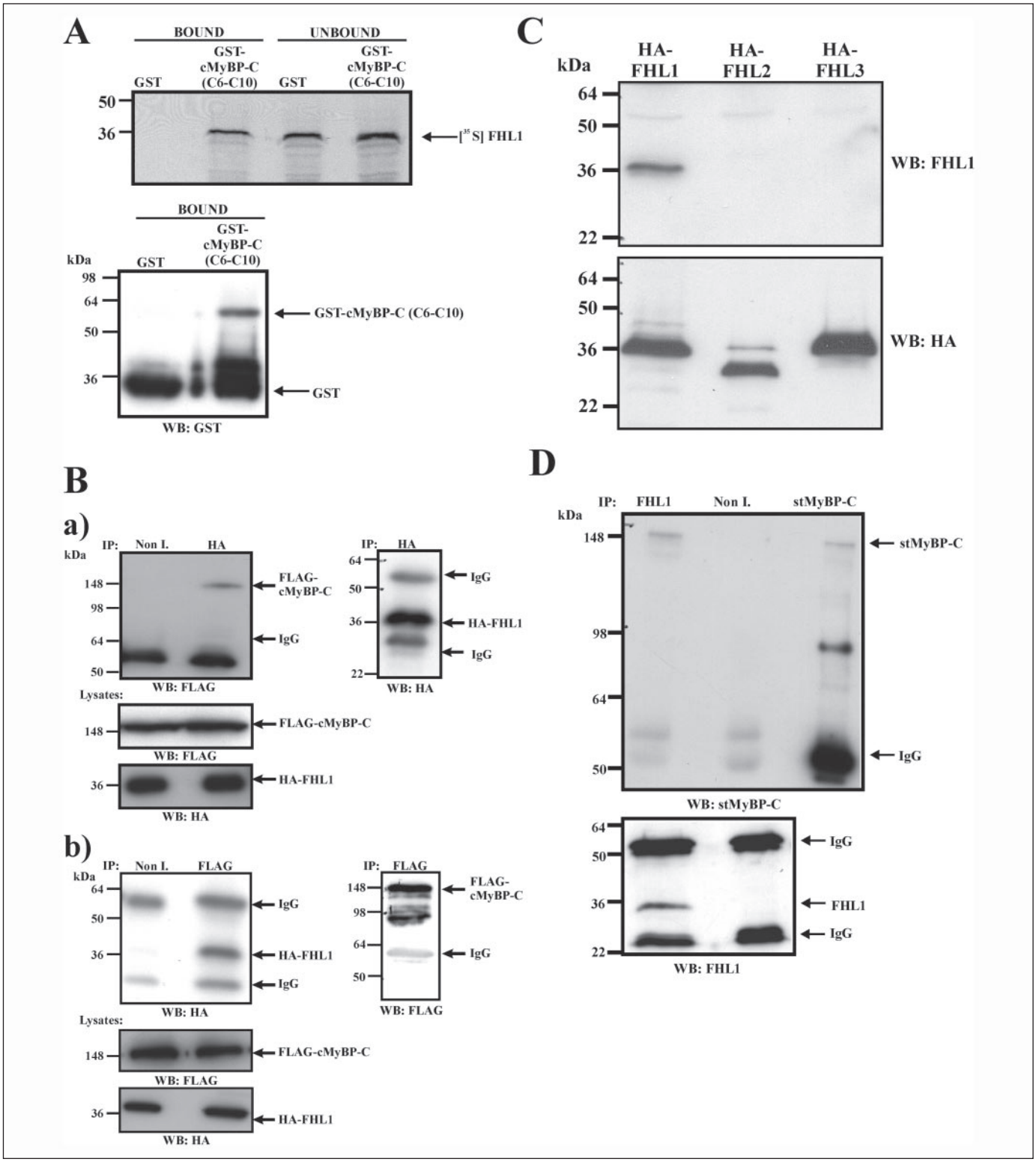

FIGURE 2. **FHL1 and MyBP-C associate *in vitro* and *in vivo*.** *A, in vitro* binding assay. GST-cardiac MyBP-C domains C6–C10 (*GST-cMyBP-C* (*C6–C10*)) and GST alone were bound to glutathione-Sepharose and mixed with *in vitro* translated ^{35}S-FHL1. Unbound and bound fractions were separated by SDS-PAGE with autoradiography to detect ^{35}S-FHL1 (*upper panel*). Bound fractions were also immunoblotted with anti-GST antibodies (*lower panel*). *B,* co-immunoprecipitation of HA-FHL1 and FLAG-cMyBP-C. Full-length HA-FHL1 and FLAG-cMyBP-C were co-expressed in COS-1 cells. *a,* lysates were immunoprecipitated with nonimmune (Non I) or HA antibodies and immunoblotted with a FLAG antibody (*upper left*). Immunoprecipitation of HA-FHL1 was confirmed by immunoblotting with anti-HA (*right*). Protein expression was confirmed by immunoblotting lysates with HA and FLAG antibodies (*lower left*). *b,* in the reciprocal experiment, lysates were immunoprecipitated (*IP*) with nonimmune or FLAG antibodies and immunoblotted (Western blot (*WB*)) with an HA antibody (*upper left*). FLAG-cMyBP-C was immunoprecipitated and immunoblotted with anti-FLAG (*right panel*). *C,* specificity of FHL1 antibody. COS-1 cells were transiently transfected with HA-FHL1, HA-FHL2, or HA-FHL3. Triton-soluble lysates were separated by SDS-PAGE and immunoblotted with either the affinity-purified FHL1 antibody (*upper panel*) or an HA antibody (*lower panel*). *D,* co-immunoprecipitation of endogenous FHL1 and stMyBP-C. Sol8 skeletal myotube lysates were immunoprecipitated with FHL1, nonimmune or stMyBP-C antibodies, and immunoblotted with a stMyBP-C antibody (*upper panel*). To confirm immunoprecipitation of FHL1, precipitates were also immunoblotted with a, FHL1 antibody (*lower panel*).

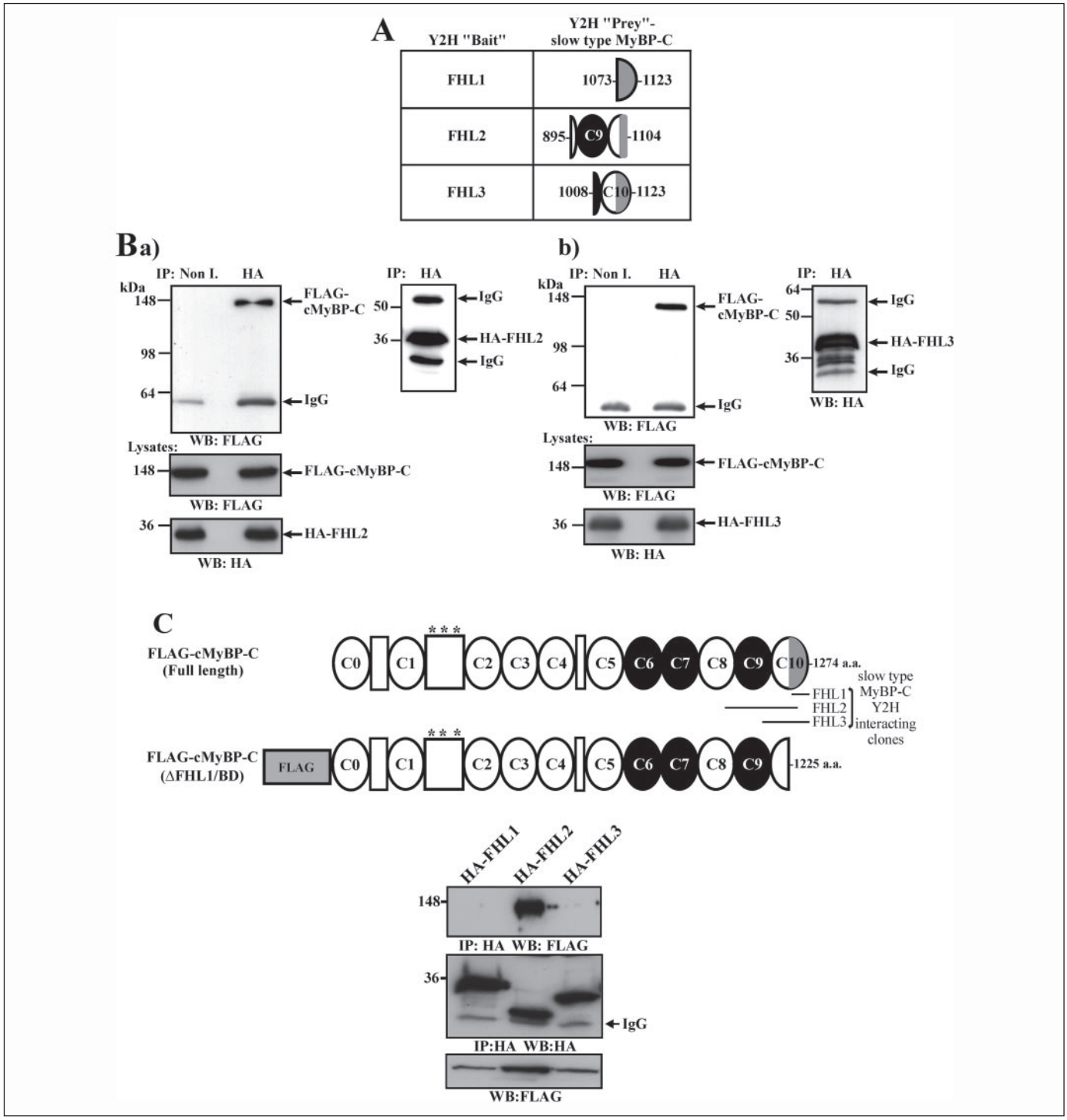

FIGURE 3. **FHL1, FHL2, and FHL3 associate with C terminus of MyBP-C.** *A,* domains of stMyBP-C bound by FHL1, FHL2, and FHL3 ("*bait*") in Y2H screen with amino acid numbers indicated. *B, a,* HA-FHL2 and FLAG-cardiac MyBP-C co-transfected COS-1 cells lysates, immunoprecipitated (*IP*) with nonimmune or anti-HA, and immunoblotted (Western blot (*WB*)) with anti-FLAG (*upper left*). Immunoprecipitation of HA-FHL2 was confirmed by immunoblotting with anti-HA (*right*). Protein expression was confirmed by immunoblotting lysates with anti-HA and anti-FLAG (*lower left*). *b,* HA-FHL3 and FLAG-cMyBP-C co-transfected cell lysates immunoprecipitated with nonimmune or anti-HA and immunoblotted with a FLAG antibody (*upper left*). *C,* domain structure of cardiac MyBP-C, containing an additional IgC2 domain (C0) and unique phosphorylation sites (*asterisk*). The C-terminal 50 amino acids corresponding to those bound by FHL1 in the Y2H screen are indicated (*gray*). FLAG-cMyBP-C (ΔFHL1/BD) is a truncation mutant lacking these C-terminal 50 amino acids. COS-1 cells were co-transfected with FLAG-cMyBP-C(ΔFHL1/BD) and either HA-FHL1, HA-FHL2. or HA-FHL3. *Upper blot*, lysates were immunoprecipitated with anti-HA and immunoblotted (*WB*) with anti-FLAG. *Middle,* immunoblotting with an HA antibody confirmed precipitation of FHL proteins. *Lower,* expression of FLAG-cMyBP-C(ΔFHL1/BD) was confirmed by immunoblotting lysates with anti-FLAG.

ity to bind FHL2. The isolated C10 domain was unstable when expressed in COS-1 cells and could not be used to demonstrate an interaction with the FHL proteins. Similar problems with the instability of MyBP-C truncation mutants have been reported previously (37).

FHL1 Impairs Binding of MyBP-C to Myosin Filaments in an in Vitro Co-sedimentation Assay—Given that the C10 domain of MyBP-C binds both FHL1 and myosin, we investigated whether FHL1 competes with myosin for binding to MyBP-C. To test this hypothesis, an *in vitro*

biochemical approach using purified myosin, recombinant FHL1, and MyBP-C was employed. Previous studies have demonstrated that purified myosin filaments pellet following high speed centrifugation (28, 38). In the absence of myosin, MyBP-C is retained exclusively in the supernatant fraction and co-sediments to the pellet only in the presence of myosin filaments (28, 38). To examine the effect of FHL1 on the binding of MyBP-C to myosin, purified His-cMyBP-C (domains C6–C10) was incubated with reconstituted myosin filaments in the presence of GST-FHL1 or GST-alone. Only domains C6–C10 of cardiac MyBP-C were used in this assay as MyBP-C contains multiple myosin binding domains at the N and C termini, although the C10 domain is the primary myosin-binding site (27–29, 31). In the presence of GST-alone, MyBP-C co-sedimented with myosin filaments (Fig. 4*A*). However, in the presence of GST-FHL1 a significant reduction in the amount of MyBP-C co-sedimenting with myosin was observed, associated with increased retention of MyBP-C in the supernatant (Fig. 4*A*). Repeat experiments allowed quantification by densitometric analysis of the relative MyBP-C protein band intensities in the pellet faction, indicating GST-FHL1 mediated a 50% reduction in the amount of MyBP-C pelleting with myosin (Fig. 4*B*).

FHL1 Shows Partial Co-localization with MyBP-C in Skeletal Muscle Sections—The localization of FHL1 in mature skeletal muscle has not been reported previously. In longitudinal sections of murine soleus muscle, staining with affinity-purified FHL1 antibody demonstrated a transverse banding pattern of alternating thick and thin bands (*arrowheads*) and staining along the sarcolemma (*arrow*) (Fig. 5*A, b–d*). This staining pattern suggests FHL1 may localize to the I-band/Z-line (thick band) and to the M-line (thin band). However, localization of FHL1 to the M-line (Fig. 5*A, c* and *d, arrowheads*) was variable and in some instances was not detected (Fig. 5*A-e*), suggesting FHL1 localization to the M-line may be transient. In transverse sections FHL1 staining was concentrated at the periphery of the fiber at the sarcolemma and subsarcolemmal region (*arrow*) (Fig. 5*A, g* and *h*). Preimmune serum was nonreactive (Fig. 5*A*, *a*).

To confirm the localization of FHL1, sections were co-stained with antibodies specific for α-actinin (Z-line), vinculin (I-band/costamere), or myosin heavy chain (MyHC) (A-band) (46–48). In low magnification images of longitudinal sections, FHL1 and α-actinin co-localized at the Z-line (Fig. 5*B, c*). However, in high magnification images, FHL1 staining appeared broader than α-actinin staining at the Z-lines (Fig. 5*B, d* and *e*). This suggests FHL1 may span a region encompassing both the I-band and Z-line. In transverse sections, FHL1 and α-actinin co-localized at the sarcolemma (Fig. 5*B, h*). The localization of α-actinin at the sarcolemma in transverse sections is consistent with a previous report in which α-actinin was detected in the detergent-insoluble, sarcolemmal membrane fraction, prepared following subcellular fractionation of myofibrils (49). Furthermore, α-actinin staining has also been observed in isolated sarcolemma that were mechanically peeled from skeletal muscle fibers (50). We have also previously detected α-actinin at the sarcolemma using immunohistochemistry of transverse skeletal muscle sections (21).

A distinct region of subsarcolemmal FHL1 staining did not co-localize with α-actinin and may represent FHL1 at the costamere (Fig. 5*B, i, arrows*). Costameres are a subsarcolemmal, cytoskeletal network that links the Z-lines (and M-lines) to the sarcolemma and extracellular matrix (51). Costameres maintain myofiber integrity during muscle contraction, anchor the sarcomere, and transmit signals from the extracellular matrix to the sarcomere and nucleus. In longitudinal sections, the costamere is detected at the I-band, consistent with the localization observed for FHL1 in longitudinal sections.

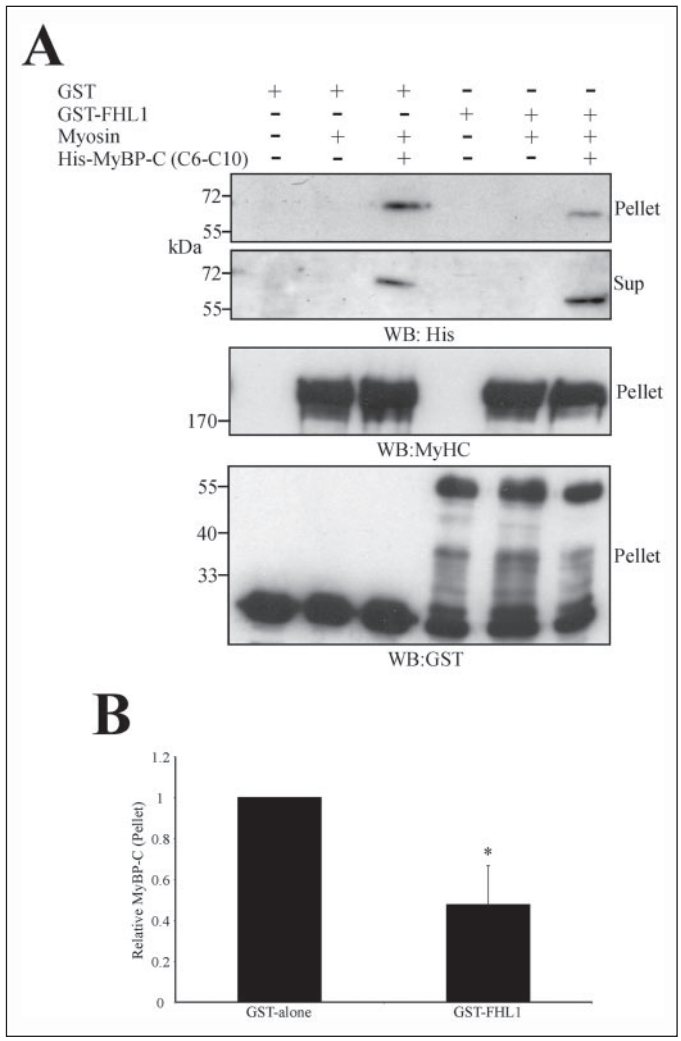

FIGURE 4. **FHL1 impairs binding of MyBP-C to myosin filaments in an *in vitro* co-sedimentation assay.** *A,* co-sedimentation assays were performed by incubating 0. 5 μM synthetic myosin filaments, 0.2 μM His-cMyBP-C domains C6–C10, and 0.5 μM of either GST alone or GST-FHL1 as indicated, overnight at 4 °C. In control studies binding buffer (20 mM imidazole, 10 mM reduced glutathione, 0.1 M KCl, pH 7.0, 1 mM dithiothreitol) was used in lieu of recombinant protein. Myosin filaments were recovered by centrifugation followed by removal of the supernatant and reconstitution of filaments (*pellet*) in SDS-PAGE reducing buffer. Pellet fractions were separated by SDS-PAGE and immunoblotted with MyHC, GST, or polyhistidine antibodies as indicated. In control studies to detect MyBP-C not bound to myosin filaments, the supernatant fraction (*Sup*) was also immunoblotted (Western blot (*WB*)) with a polyhistidine antibody. *B,* the amount of MyBP-C (*pellet*) co-sedimenting and therefore binding to myosin filaments was measured using densitometry. The amount of bound MyBP-C in the presence of GST-FHL1 was determined relative to GST alone, which was arbitrarily assigned a value of 1. Data represent the mean from three independent experiments (± S.E.). *, $p < 0.05$.

To confirm that FHL1 localizes within the I-band, sections were co-stained with FHL1 and vinculin. Vinculin was detected at the I-band and sarcolemma in longitudinal and transverse sections, respectively, consistent with its reported localization at the costamere (Fig. 5*B, k* and *o*) (47). FHL1 co-localized with vinculin in both longitudinal and transverse sections (Fig. 5*B, l, m, p,* and *q*).

The M-line is located at the center of the sarcomere, flanked on either side by the A-band, and is the anchorage point for myosin thick filaments (48). To verify that a pool of FHL1 also localizes to the M-line, co-localization studies were performed using a myosin heavy chain antibody (MyHC). The MyHC antibody showed thick but faint staining at the A-band, with more intense staining at the M-line (Fig. 5*B, s*). The thin intervening band of FHL1 staining co-localized with MyHC at the

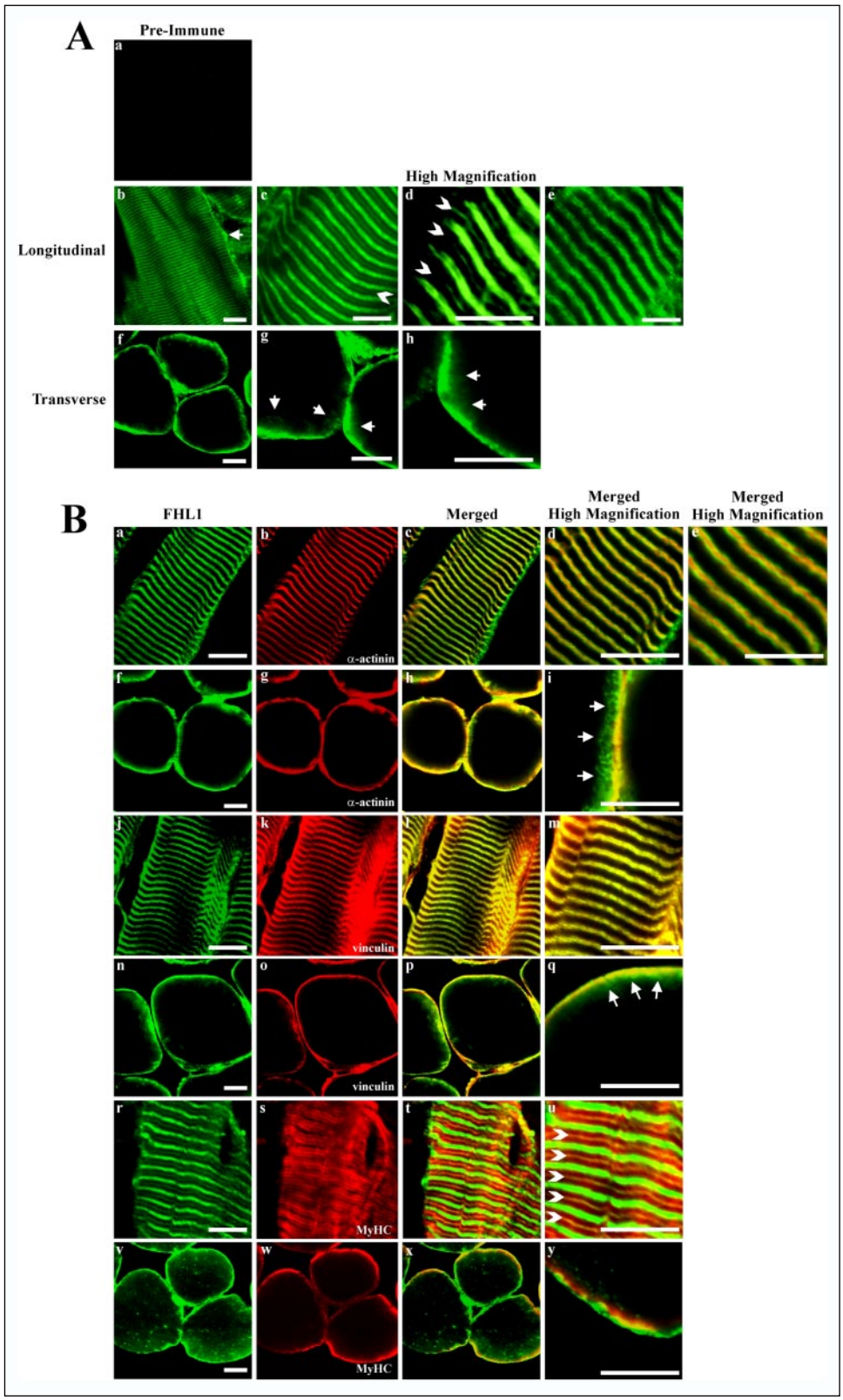

FIGURE 5. **FHL1 localizes to the sarcolemma, Z-line/I-band region, and M-line in mature skeletal muscle and isolated myofibrils.** FHL1 partially co-localizes with MyBP-C. *A–C*, immunohistochemistry of longitudinal and transverse cryosections from mouse soleus muscle, viewed using laser scanning confocal microscopy. *A*, longitudinal (*a–e*) or transverse (*f–h*) sections stained with an FHL1 antibody (*b–h*) or preimmune serum (*a*). Images in *d* and *h* are high magnification. *b*, *arrow* indicates FHL1 staining along sarcolemma; *g* and *h* indicate subsarcolemmal staining. *Arrowhead* in *c* and *d* indicate thin intervening band of staining (*M-line*). In longitudinal skeletal muscle sections FHL1 localizes to an alternating pattern of thick (Z-line/I-band) and thin (M-line) bands. Localization of FHL1 to the M-line (*c* and *d*) is variable and in some instances was not detected (*e*). In transverse sections FHL1 localizes to the sarcolemma and sub-sarcolemmal regions (*g* and *h*). *B*, longitudinal (*a–e*, *j–m*, and *r–u*) or transverse (*f–i*, *n–q*, and *v–y*) sections co-stained with FHL1 (*green*) and either α-actinin, vinculin, or MyHC antibodies as indicated. Merged and high magnification images are also as indicated. *Arrows* in *i* and *q* indicate sub-sarcolemmal FHL1 staining. *Arrowheads* in *u* indicate FHL1 M-line staining overlying MyHC within the A-band region. *C*, longitudinal (*a–c*) or transverse (*d–g*) sections co-stained with FHL1 and slow type skeletal MyBP-C antibodies. Note, images in *a–c* and *g* are high magnification. *Scale bar* 50 μm, 25 μm in high magnification images (15 μm image *B*, *e*). *D*, myofibrils isolated from murine skeletal muscle were stained with an FHL1 antibody (*a–e*). FHL1 localizes to an alternating pattern of thick (*arrows*) (I-band) and thin (*arrowheads*) (M-line) bands. This was confirmed by comparing the immunofluorescence (*upper panel*) and bright field (*lower panel*) images (*c*) of a single isolated myofibril. The thick and thin bands of FHL1 staining in the immunofluorescence image correspond to the isotropic (I-band) and center of the anisotropic (A-band) regions, respectively, in the bright field image. Localization of FHL1 to the M-line (*arrowheads*) is variable, ranging from totally absent in some myofibrils (*b*) to a thin intervening band (*a* and *d*) or a broad intensely staining band (*e*). Myofibrils were also co-stained (*f–q*) with an FHL1 antibody and either α-actinin, vinculin, or MyHC as indicated. *d*, *e*, *i*, *m*, and *q*, three-dimensional blind deconvolved confocal microscopy images. *Arrows* indicate I-band, and *arrowheads* indicate *M-line*. *E*, myofibrils were co-stained with a slow type skeletal MyBP-C antibody and either FHL1, FHL2, or FHL3 antibodies as indicated. *d*, *h* and *l*, three-dimensional blind deconvolved confocal microscopy images. *Scale bar*, 25 and 10 μm deconvolved images.

M-line (Fig. 5*B*, *t* and *u*, *arrowheads*). In transverse sections, FHL1 and MyHC localized to adjacent regions, with a distinct region of overlapping staining at the subsarcolemma (Fig. 5*B*, *x* and *y*).

Immunoelectron microscopy indicates that MyBP-C localizes to the C-zone (cross-bridge) within the A-band and appears as a doublet that flanks either side of the M-line (26, 52, 53). The co-localization of MyBP-C and FHL1 was examined in longitudinal sections from stretched soleus muscle. Consistent with a previous report, MyBP-C localized to a doublet in longitudinal sections (Fig. 5*C*, *b*) (54). Partial co-localization between FHL1 and MyBP-C was apparent at the periphery of the I-band (Fig. 5*C*, *c*). FHL1 and MyBP-C also co-localized in transverse sections at the sarcolemma/subsarcolemma (Fig. 5*C*, *f* and *g*).

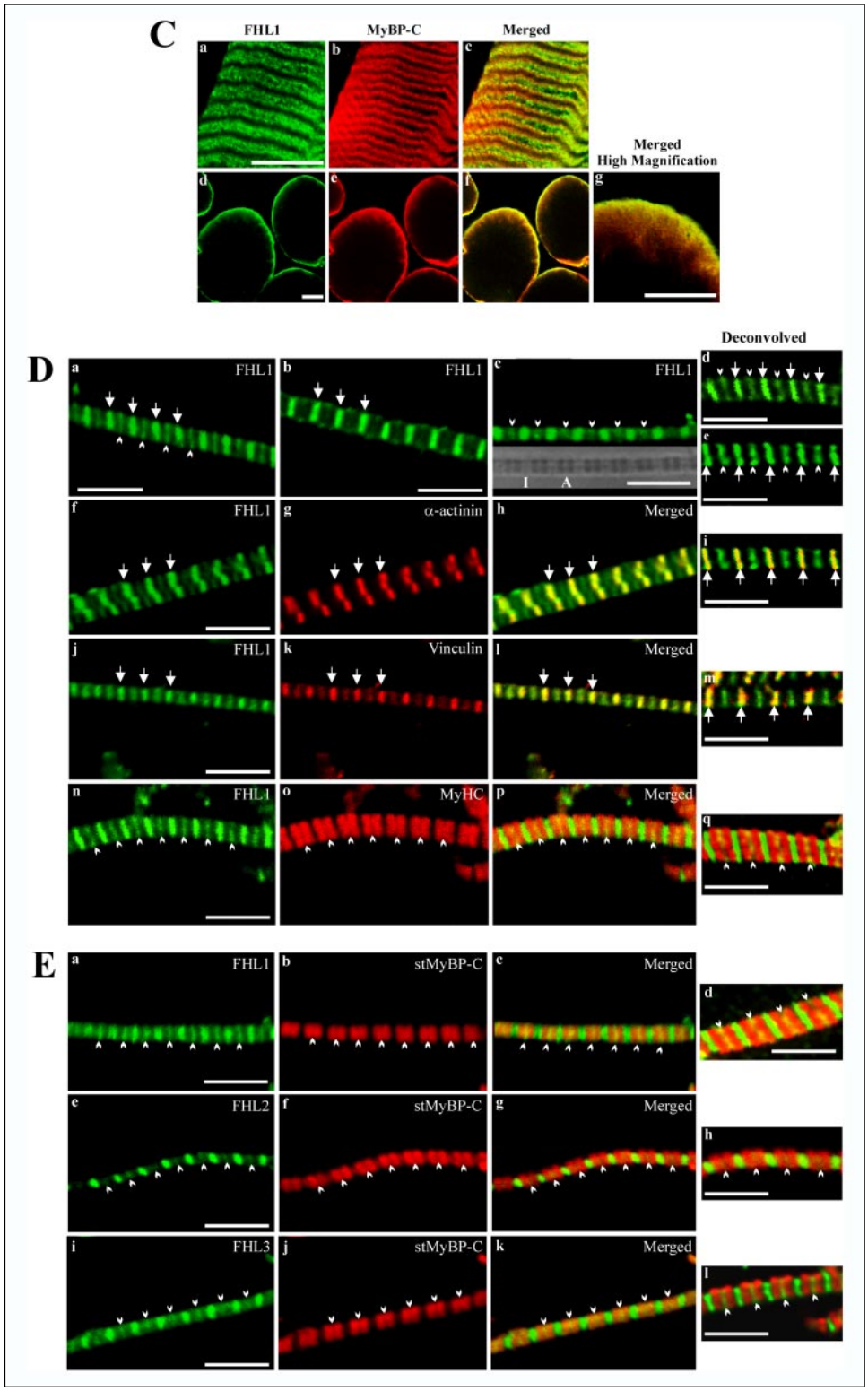

FIGURE 5—*continued*

However, imaging using the MyBP-C antibody in longitudinal sections of stretched skeletal muscle was consistently not as definitive as observed in isolated myofibrils (see below).

Localization of FHL1 in Isolated Skeletal Myofibrils and Partial Co-localization with MyBP-C—To define further the localization of FHL1 in skeletal muscle, individual myofibrils were isolated by homogenization and stained with the FHL1 antibody alone or co-stained with α-actinin, vinculin, MyHC, or slow type MyBP-C antibodies (Fig. 5, *D* and *E*). To more precisely discern individual sarcomeric structures, three-dimensional blind deconvolution was also employed to permit high magnification and resolution imaging. In a previous study, distributed deconvolution was used to measure the thin filament lengths of isolated myofibrils with a precision comparable with electron microscopy (55).

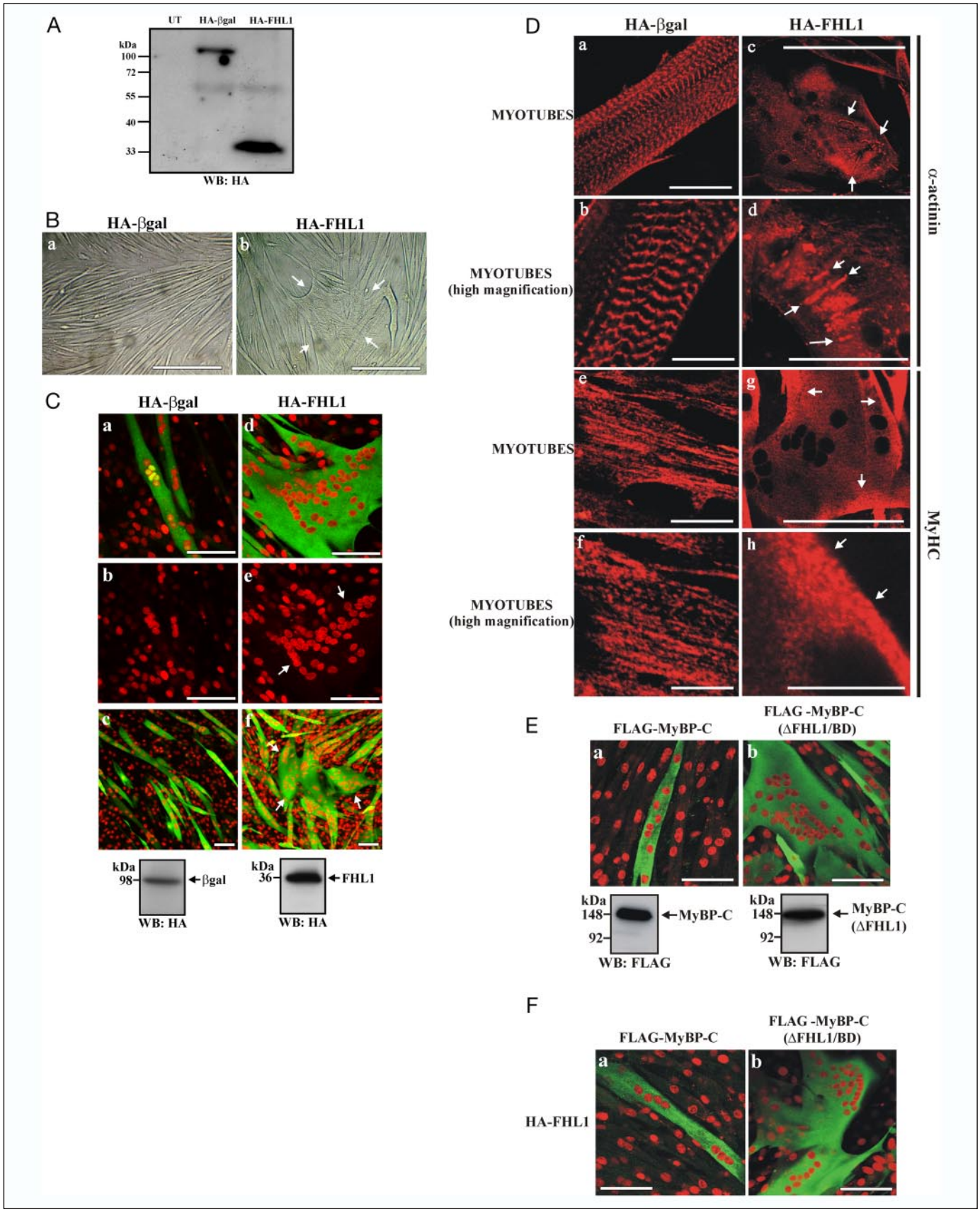

FIGURE 6. **Overexpression of FHL1 in differentiating C2C12 cells induces multinucleated myosac formation and impairs Z-line and myosin thick filament assembly.** *A,* lysates from untransfected (*UT*) and stably transfected C2C12 cells expressing HA-βgal or HA-FHL1 were separated by SDS-PAGE and immunoblotted with an HA antibody. *B,* bright field images of stably transfected C2C12 cells expressing HA-βgal or HA-FHL1 induced to differentiate for 96 h. *Arrows* in *b* indicate myosacs. *C,* C2C12 myoblasts were transiently transfected with either HA-βgal (*a–c*) or HA-FHL1 (*d–f*) and induced to differentiate for 96 h. HA-tagged proteins were detected by staining with an HA antibody (*green*), and cells were

FHL1 localized to the I-band and M-line in isolated skeletal myofibrils (Fig. 5*D, a*), consistent with the staining pattern observed in skeletal muscle longitudinal sections (Fig. 5*A, c* and *d*). As observed in skeletal muscle sections, FHL1 staining at the M-line in myofibrils was variable ranging from totally absent in some myofibrils (Fig. 5*D, b*) to a thin intervening band (Fig. 5*D, a* and *d, arrowheads*) or a broad intensely staining band (Fig. 5*D, e*, *arrowheads*). This staining pattern was confirmed by comparing the immunofluorescence (*upper panel*) and bright field (*lower panel*) images of a single isolated myofibril (Fig. 5*D, c*). The thick and thin bands of the immunofluorescence image correspond to the isotropic (I-band) and center of the anisotropic (A-band) regions, respectively, in the bright field image.

FHL1 co-localized with both α-actinin (Fig. 5*D, h* and *i*) and vinculin (Fig. 5*D, l* and *m*) in the Z-line/I-band region (*arrows*). Immunofluorescence studies in isolated somites have demonstrated that MyHC staining appears as a doublet within the A-band that flanks either side of the central unstained M-line (54). In isolated myofibrils, we observed that FHL1 staining at the M-line localized central to the MyHC doublet (Fig. 5*D, n–p, arrowheads*). However, in the high magnification and high resolution deconvolved images FHL1 staining showed partial co-localization with MyHC (Fig. 5*D-q*, *arrowheads*). This suggests FHL1 staining at the M-line may also extend partially into the C-zone, a region of the A-band just adjacent to the M-line.

Consistent with this contention, FHL1 staining at the M-line also partially co-localized with MyBP-C, which previous reports indicate localizes to a doublet at the C-zone within the A-band (Fig. 5*E, c* and *d, arrowheads*) (56). The co-localization of other FHL proteins with MyBP-C was also determined. FHL3 localized predominantly to the Z-line and was also detected at the M-line (Fig. 5*E, i, arrowheads*) but did not co-localize with MyBP-C. Similarly FHL2 staining was detected predominantly at the Z-line, and no staining was noted at the M-line in skeletal myofibrils (Fig. 5*E, e, arrowheads*), and co-localization with MyBP-C was not evident (Fig. 5*D, g* and *h, arrowheads*).

Overexpression of FHL1 in Differentiating Skeletal C2C12 Cells Impairs Z-line and Myosin Thick Filament Assembly—To investigate the functional consequences of complex formation between FHL1 and MyBP-C, we undertook studies examining the effect of FHL1 overexpression or RNAi-mediated knockdown of FHL1 expression in differentiating C2C12 skeletal myoblasts. Myoblasts stably overexpressing HA-FHL1 or HA-βgal were generated, and protein expression was confirmed by immunoblotting with an HA antibody (Fig. 6*A*). Significantly, when induced to differentiate C2C12 cells stably expressing HA-FHL1 demonstrated greatly enlarged "sac-like" myotubes (named myosacs) (Fig. 6*B*, *b, arrows*) that were not observed in differentiating myotubes expressing HA-βgal (Fig. 6*B*, *a*). These myosacs were also observed in C2C12 cells transiently transfected with HA-FHL1 and induced to differentiate, but not control cells transfected with HA-βgal (Fig. 6*C*), which formed long thin myotubes, with a linear arrangement of nuclei (Fig. 6*C, a–c*). In contrast, HA-FHL1 expressing myosacs contain large crowded clusters of nuclei (Fig. 6*C, d–f, arrows*). Other LIM-only proteins including FHL2, FHL3, and muscle LIM protein (MLP) are highly expressed in skeletal muscle (1, 57). Overexpression of FHL2 promotes myoblast differentiation via inhibition of Wnt signaling; however, myosac formation was not reported (16). Similarly, myosac formation was not demonstrated in differentiating myoblasts expressing muscle LIM protein, which promotes myogenesis by binding the myogenic regulatory transcription factor MyoD (58). In control studies we did not detect myosacs upon FHL3 overexpression in differentiating C2C12 myoblasts (data not shown).

The term "myosacs" has been used to describe a phenotype of enlarged sac-like myotubes (59–68). The formation of myosacs has been associated previously with impaired sarcomere formation during myofibrillogenesis, whereby the disrupted or compromised cytoskeleton results in retraction of the growth tip of the myotube to form a sac-like myotube or myosac (59–61, 63, 64). Most interestingly, expression of mutant MyBP-C that lacks the C-terminal C10-myosin binding domain in skeletal myotubes and cardiomyocytes potently inhibits sarcomere formation (37, 38). We characterized the effect of FHL1 expression on sarcomere formation by examining Z-line assembly (α-actinin staining) and myosin thick filament assembly by staining with a myosin antibody (MF20), the epitope of which has been mapped previously to the LMM region of myosin heavy chain (69). HA-βgal control expressing myotubes demonstrated a striated α-actinin staining pattern, indicating formation and alignment of the Z-line (Fig. 6*D, a* and *b*). However, in HA-FHL1 expressing myotubes, α-actinin staining was diffusely cytoplasmic and formed only occasional, irregular, linear aggregations (*arrows*), suggesting Z-line formation may be delayed or disrupted (Fig. 6*D, c* and *d*). Myosin thick filament assembly was also disrupted by FHL1 overexpression, as myosin striations were not observed, and myosin was distributed diffusely in the cytoplasm, with increased staining intensity at the cell periphery (Fig. 6*D, g* and *h, arrows*). HA-βgal expressing myotubes exhibited a linear, striated arrangement of myosin, indicative of early thick filament formation (Fig. 6*D, e* and *f*).

The functional relationship between FHL1, MyBP-C, and myosac formation was investigated. Differentiating C2C12 cells were transfected with either full-length FLAG-cMyBP-C or truncated cMyBP-C, which lacks the FHL1 binding domain on C10 (FLAG-cMyBP-C(ΔFHL1/BD)) (Fig. 6*E*). Myoblasts expressing full-length FLAG-cMyBP-C formed long thin myotubes with a linear arrangement of nuclei (Fig. 6*E, a*). In contrast, overexpression of FLAG-cMyBP-C (ΔFHL1/BD) induced the formation of myosacs, with crowded clusters of nuclei, a phenotype similar to that obtained upon FHL1 overexpression (Fig. 6*E*, *b*).

FHL1 binding to MyBP-C may impair MyBP-C association with myosin, resulting in myosin thick filament disruption and/or dysregulation. We reasoned co-expression of full-length FLAG-cMyBP-C, but not truncated FLAG-cMyBP-C(ΔFHL1/BD), may rescue the FHL1-induced myosac phenotype, if FHL1 is competing with myosin for MyBP-C. To this end, C2C12 cells stably expressing HA-FHL1 were co-transfected with either full-length FLAG-cMyBP-C or FLAG-cMyBP-C(ΔFHL1/BD) (Fig. 6*F*). Co-expression of full-length FLAG-

co-stained with propidium iodide to detect nuclei (*red*). *Arrows* in *f* indicate myosacs. Expression of recombinant protein was confirmed by immunoblotting lysates with anti-HA. *Scale bars,* 50 μm. *D,* C2C12 myoblasts stably expressing HA-βgal (*a, b, e,* and *f*) or HA-FHL1 (*c, d, g,* and *h*) were differentiated for 144 h and stained with antibodies to either α-actinin (*Z-line*) (*a–d*) or MyHC (thick filament) (*e–h*). *Arrows* in *c* and *d* indicate linear aggregates of α-actinin, and *arrows* in *g* and *h* indicate concentration of myosin at the membrane. *Scale bar,* 25 μm. *E* and *F,* overexpression of FHL1 induces the formation of myosacs by competing for binding to MyBP-C. To determine the molecular mechanisms mediating FHL1-induced myosac formation, the functional relationship between FHL1, MyBP-C, and myosac formation was investigated. *E,* C2C12 myoblasts were transiently transfected with either full-length FLAG-cMyBP-C (*a*) or FLAG-cMyBP-C (ΔFHL1/BD) (*b*), which lacks the FHL1-binding domain. Cells were induced to differentiate for 96 h and co-stained with a FLAG antibody (*green*) and propidium iodide (*red*) to detect nuclei. To confirm expression of recombinant proteins, cell lysates were prepared and immunoblotted with anti-FLAG. *F,* FHL1 may induce myosac formation by binding to the C terminus of MyBP-C impairing the latter's association with myosin. C2C12 cells stably expressing HA-FHL1 were co-transfected with either (*a*) full-length FLAG-cMyBP-C or (*b*) FLAG-cMyBP-C(ΔFHL1/BD) and induced to differentiate for 96 h. Cells were co-stained with anti-FLAG (*green*) and propidium iodide (*red*). Scale bars, 50 μm.

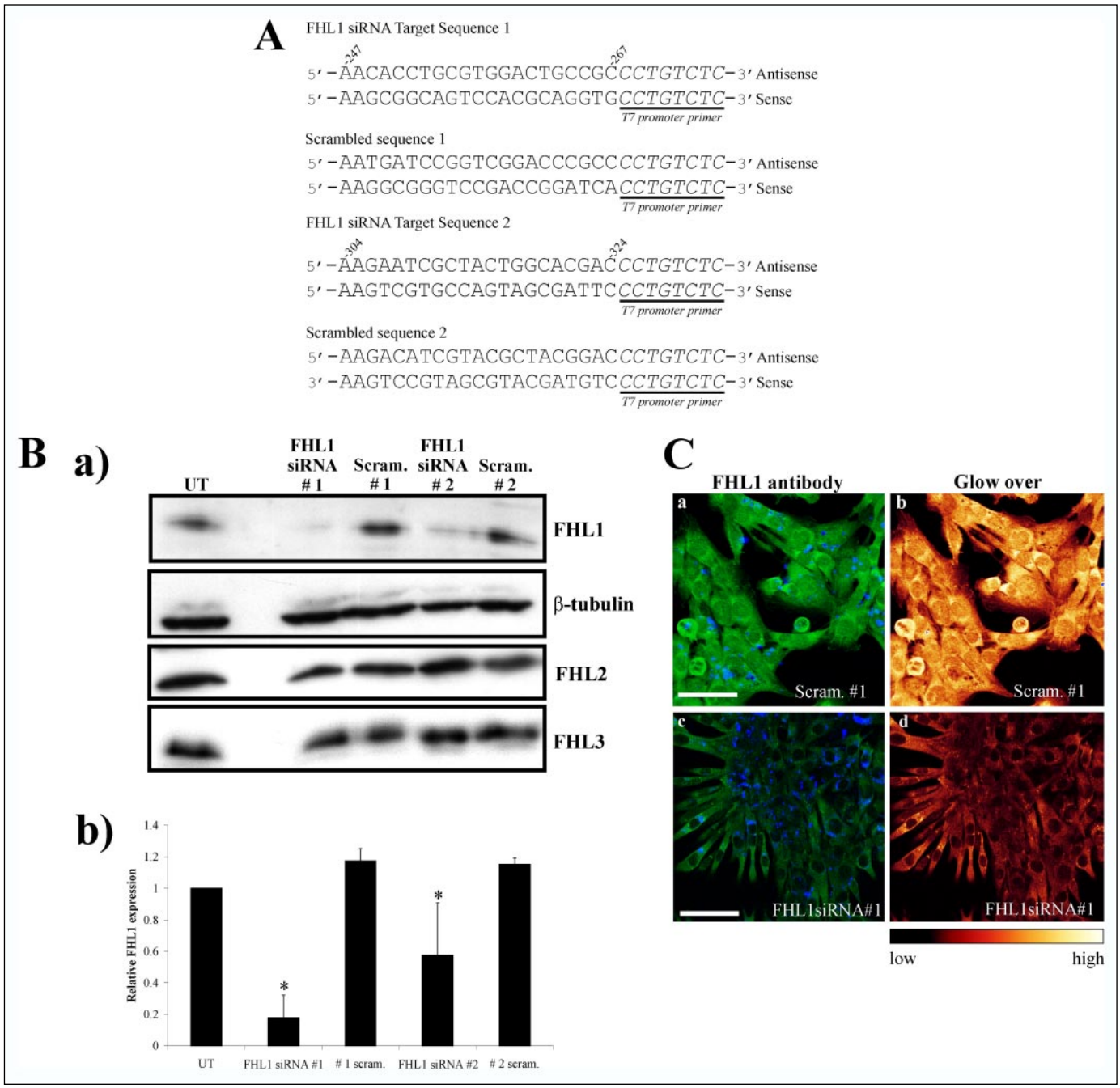

FIGURE 7. **Underexpression of FHL1 in skeletal myoblasts using RNAi.** *A,* DNA oligonucleotide sequences specific for murine FHL1 (GenBank™ accession number NM_010211) were used as templates to synthesize double-stranded siRNA. Nucleotide numbers of the two target sequences are indicated above. Sequences of control, scrambled oligonucleotides are also shown. The 8-nucleotide leader sequence to which the T7 promoter primer anneals is indicated in *italics* and *underlined. B, a,* C2C12 myoblasts were transiently transfected with 25 nM siRNA oligonucleotides corresponding to either target sequence 1 (*FHL1 siRNA # 1*), target sequence 2 (*# 2*), or scrambled siRNA oligonucleotides (*# 1 scram* or *# 2 scam*), or left untransfected (*UT*). 48 post-transfection Triton-soluble lysates were prepared and 25 μg of protein separated by SDS-PAGE and immunoblotted with antibodies specific for FHL1, β-tubulin (loading control), FHL2, or FHL3 as indicated. *b,* relative FHL1 protein expression was quantitated using densitometry. The relative expression of FHL1 in each transfection was adjusted for protein loading by comparison with β-tubulin protein levels and compared with FHL1 levels in untransfected cells, which were arbitrarily assigned a value of 1.0. The results represent the mean of three separate experiments $\pm$ S.D. *, $p < 0.05$. *C,* to confirm FHL1 protein knockdown, C2C12 myoblasts were co-transfected with either scrambled (*Scram #1*) or FHL1 (*FHL1 siRNA #1*) siRNA previously labeled with Cy5 (*blue*) and 48 h post-transfection stained with an FHL1 antibody (*green*). Cells were visualized using laser scanning confocal microscopy, and both scrambled and FHL1 siRNA transfected cells were imaged at identical laser attenuation to permit direct comparison of relative FHL1 staining intensity. Both true color (*a* and *c*) and glow over (*b* and *d*) images are presented. A scale bar depicting the range of staining intensities for glow over images is included below. *Scale bar,* 50 μm.

cMyBP-C, but not FLAG-cMyBP-C(ΔFHL1/BD), with FHL1 prevented the formation of FHL1-induced myosacs, and only thin myotubes were detected (Fig. 6*F, a* and *b*).

FHL1 Knockdown Using RNAi in Differentiating Skeletal Myoblasts Inhibits Myosin Thick Filament Assembly and Incorporation of MyBP-C into the Sarcomere—To confirm the involvement of FHL1 in the regulation of sarcomeric assembly, the effect of FHL1 RNAi knockdown was examined. Four FHL1 siRNA duplexes were synthesized and transfected into C2C12 myoblasts. Two FHL1 siRNA-specific sequences (247–275 and 304–312) (Fig. 7*A*) resulted in decreased FHL1 protein

expression as shown by immunoblot analysis, relative to FHL1 RNAi sequences scrambled or untransfected cells (Fig. 7*B*, *a*). β-Tubulin immunoblot analysis of cell lysates confirmed equal protein loading. The relative FHL1 protein level, in FHL1 siRNA 1 and 2 transfected cells decreased by 80 and 50%, respectively, compared with the corresponding scrambled sequences (Fig. 7*B*, *b*). No change in FHL2 or FHL3 protein levels were detected (Fig. 7*b*, *a*). This suggests that FHL2 and FHL3 are not up-regulated to compensate for the reduction in FHL1 protein expression.

To confirm knockdown of FHL1 protein expression, C2C12 myoblasts were co-transfected with either scrambled or FHL1 siRNA 1 labeled with Cy5 (blue), and 48-h post-transfection cells were stained with an FHL1 antibody (green). Cells were visualized using laser scanning confocal microscopy, at the same laser attenuation to permit direct comparison of relative FHL1 staining intensity. Transfection of siRNA was confirmed by the appearance of distinct blue dots within cells (Fig. 7*C*, *a* and *c*). In both true color (Fig. 7*C*, *a* and *c*) and glow over (Fig. 7*C*, *b* and *d*) images, FHL1 staining was significantly reduced in FHL1 siRNA-transfected cells relative to scrambled controls.

Sarcomeric assembly was examined in differentiating myotubes transfected with FHL1 siRNA 1 (Fig. 8*A*, *a–f*) or FHL1 siRNA 2 (data not shown) with equivalent results. Myotubes transfected with FHL1 siRNA fused to form long thin myotubes, with a linear arrangement of nuclei. Furthermore, α-actinin staining revealed a striated pattern, indicating the formation and correct alignment of the Z-line similar to scrambled siRNA-transfected myotubes (not shown). However, myosin thick filament assembly was significantly abnormal in cells transfected with FHL1 siRNA. 24 h following the induction of differentiation in scrambled siRNA myoblasts, diffuse myosin staining was detected (Fig. 8*A*, *g* and *h*). At 24 h FHL1 siRNA myoblasts demonstrated myosin staining in dense sheets throughout the cytosol (Fig. 8*A*, *a* and *b*, *arrows*). By 96 h differentiation, scrambled siRNA myotubes demonstrated a linear, striated arrangement of myosin, consistent with early thick filament formation (Fig. 8*A*, *k–l*, *arrowheads*). In contrast, in FHL1 siRNA myotubes myosin striations were not detected up to 96 h differentiation, and instead myosin persisted as dense clumps in the cytosol (Fig. 8*A*, *e* and *f*, *arrows*). This observation was confirmed by quantifying the percentage of cells demonstrating dense aggregates of myosin (Fig. 8*A*, *lower panel*). At each time interval following the induction of differentiation, a significant percentage (>80% by 96 h) of cells transfected with FHL1 siRNA exhibited dense myosin aggregates, compared with scrambled RNAi control. The failure of myosin to incorporate into the sarcomere in cells with decreased FHL1 protein expression was distinct to that observed in myotubes ectopically overexpressing FHL1, where myosin was diffusely detected in the cytosol with increased staining at the cell periphery (Fig. 6*D*, *g* and *h*).

Disruption of MyBP-C incorporation into the sarcomere was also detected in FHL1 siRNA differentiating myotubes (Fig. 8*B*). At 24, 48, and 96 h of differentiation, dense aggregates of MyBP-C were observed in FHL1 RNAi but not scrambled RNAi myotubes (Fig. 8*B*, *a–f*, *arrows*). The effect of FHL1 underexpression on MyBP-C appeared to be less dramatic than that observed for myosin, as only a maximum of 45% of cells displayed aberrant MyBP-C localization, compared with 80% of cells that displayed myosin mislocalization (Fig. 8*B*, *lower panel*).

DISCUSSION

Numerous studies have revealed FHL2 and FHL3 regulate transcription factors and actin cytoskeletal dynamics. However, no functional interaction of FHL1 with either transcription factors or cytoskeletal or signaling proteins has yet been characterized. The study reported here has identified a functionally significant interaction between the major myosin thick filament-associated protein, MyBP-C and FHL1. FHL1 and MyBP-C formed a complex as shown by direct protein binding studies and co-immunoprecipitation of recombinant and/or endogenous proteins. In addition, FHL1 inhibited the association of MyBP-C with myosin filaments using *in vitro* co-sedimentation assays. This suggests FHL1 and myosin may compete for binding to MyBP-C.

FHL1 overexpression in differentiating skeletal myoblasts induced the formation of multinucleated myosacs, associated with disruption of the Z-line and myosin thick filaments. The development of FHL1-induced myosacs was rescued by co-expression of MyBP-C, suggesting that FHL1 competes with myosin for binding to MyBP-C, and as a consequence disrupts sarcomere formation. In addition, RNAi-mediated knockdown of FHL1 was associated with impaired myosin thick filament formation and incorporation of MyBP-C into the sarcomere. Collectively, this study has identified FHL1 as a novel regulator of MyBP-C activity and sarcomere assembly. Although we have demonstrated here that both FHL1 overexpression and RNAi-mediated knockdown are associated with significant abnormalities in myofibrillogenesis, given the other FHL family members bind multiple proteins, we cannot exclude the possibility that FHL1 also has multiple binding partners, including transcription factors and cytoskeletal proteins, in addition to MyBP-C, that may contribute to its function in regulating skeletal muscle differentiation.

FHL1 Localizes to the I-band/Z-line and M-line of Skeletal Muscle Where It Partially Co-localizes with MyBP-C—The localization of FHL1 in mature skeletal muscle has not been reported previously. We have demonstrated in this study that FHL1 localizes to the I-band/Z-line region and to the M-line in both mature skeletal muscle sections and isolated myofibrils. As reported previously FHL2 also localizes to the I-band and faintly to the M-line in isolated cardiomyocytes, where it binds titin and scaffolds several muscle metabolic enzymes (70). We have shown previously that FHL3 localizes to the Z-line in intact, mature skeletal muscle where it binds skeletal α-actin (21).

We noted using deconvolution microscopy that FHL1 staining at the M-line also appeared to partially extend into the C-zone of the A-band where it co-localized with MyBP-C. Moreover, we also observed that localization of FHL1 to the M-line was variable, suggesting that either the association of FHL1 and MyBP-C may be regulated or transient or that the FHL1 antibody epitope is masked. Interestingly, we have also noted co-localization between FHL1 and MyBP-C within the sarcomere of regenerating soleus skeletal muscle following cardiotoxin injection (not shown).

In transverse sections of intact skeletal muscle FHL1 was concentrated at the sarcolemma and subsarcolemma. The costamere is a subsarcolemmal cytoskeletal network that is detected at the I-band in longitudinal sections, consistent with the localization observed here for FHL1 (51). The costamere is the myofiber equivalent of focal adhesions, and many focal adhesion-associated proteins, including talin, α-actinin, focal adhesion kinase, and vinculin, localize to costameres (71). Integrins also localize to costameres where they form a mechanical link between the basal lamina and sarcomere via the costamere (48, 72). Consistent with this contention, we have previously demonstrated that FHL1 localizes to focal adhesions in skeletal myoblasts, where it promotes integrin-dependent cell spreading and migration (43).

FHL1 Regulates Sarcomere Formation during Myogenesis—We propose FHL1 competes with myosin for binding to MyBP-C. Indeed, in an *in vitro* assay FHL1 reduced co-sedimentation and hence binding of MyBP-C to myosin filaments. Interestingly, expression of MyBP-C lacking the C10 domain in skeletal myotubes and cardiomyocytes potently inhibits sar-

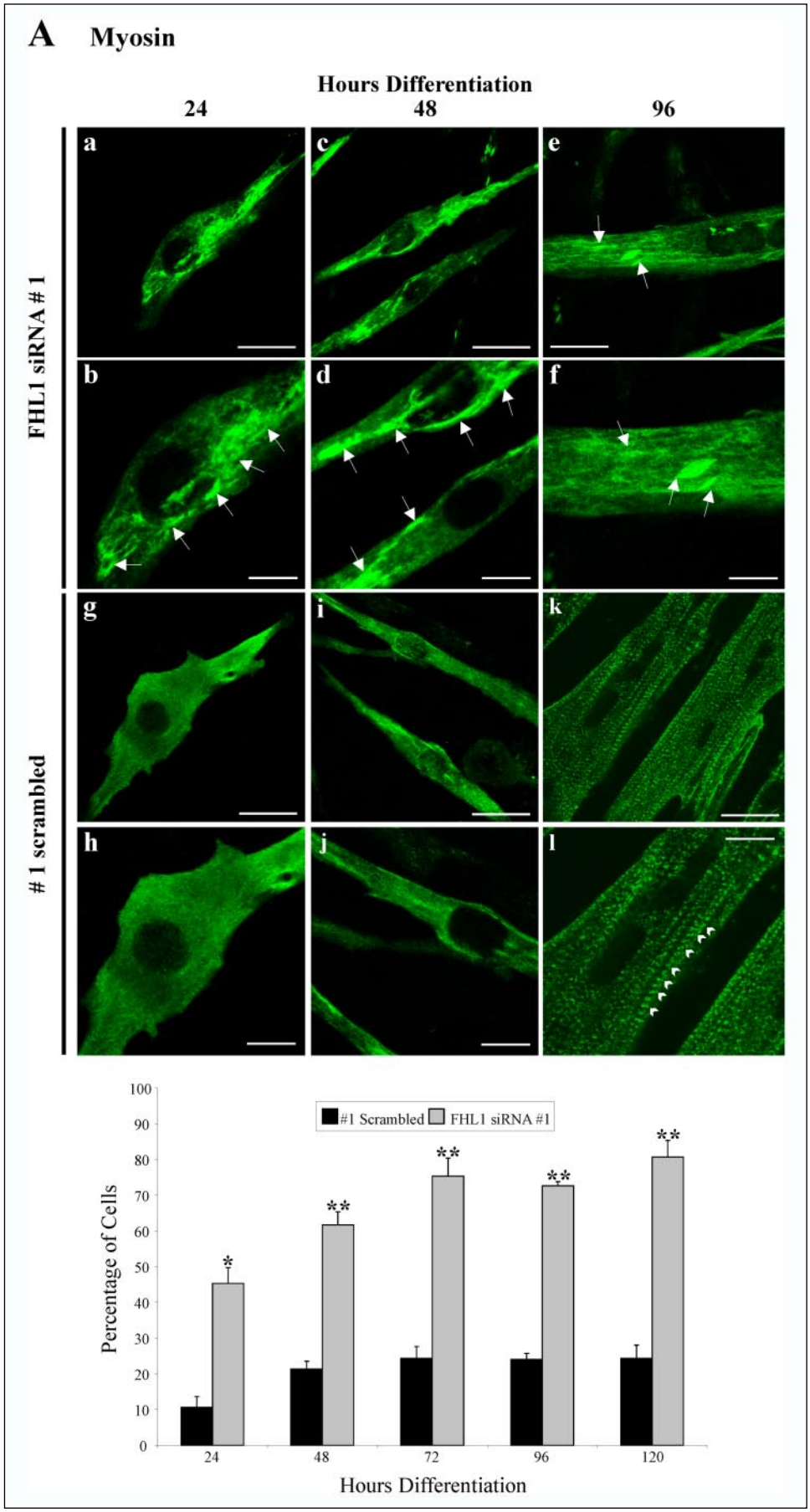

FIGURE 8. **FHL1 knockdown in differentiating skeletal myoblasts inhibits myosin and MyBP-C assembly into the sarcomere.** *A, upper,* C2C12 myoblasts were transiently transfected with 25 nM siRNA oligonucleotides corresponding to target sequence 1 (*FHL1 siRNA # 1*) (*a–f*) or a scrambled sequence (*# 1 scrambled*) (*g–l*). 48 h post-transfection myoblasts were induced to differentiate for 24–96 h as indicated. Cells were stained with an MyHC antibody followed by anti-mouse FITC-conjugated secondary antibody (*green*). *Arrows* in *b, d,* and *f* indicate dense myosin staining; *arrowheads* in *l* indicate early myosin striations. *Scale bar,* 25 μm, 10 μm high magnification images (*b, d, f, h, j,* and *l*). *Lower,* the percentage of cells exhibiting dense aggregates of myosin was quantitated for both scrambled and FHL1 siRNA-transfected cells, following induction of differentiation from 24 to 120 h as indicated. Data represent the mean from three independent experiments (± S.E.) (100 cells scored per experiment). *, $p < 0.05$; **, $p < 0.001$. *B, upper,* C2C12 myoblasts were transiently transfected with 25 nM siRNA oligonucleotides corresponding to *FHL1 siRNA #1* (*a–f*) or scrambled sequence (*#1 scrambled*) (*g–l*). 48 h post-transfection myoblasts were induced to differentiate for 24–96 h as indicated and stained with a slow type MyBP-C antibody followed by anti-mouse FITC-conjugated secondary antibody (*green*). *Arrows* in *a–f* indicate dense MyBP-C staining. *Scale bar,* 25 μm, 10 μm high magnification images (*b, d, f, h, j,* and *l*). *Lower,* the percentage of cells exhibiting dense aggregates of MyBP-C was quantitated for both scrambled and FHL1 siRNA-transfected cells, following induction of differentiation from 24 to 120 h as indicated (100 cells scored per experiment). Data represent the mean from three independent experiments (± S.E.). *, $p < 0.05$; **, $p < 0.001$.

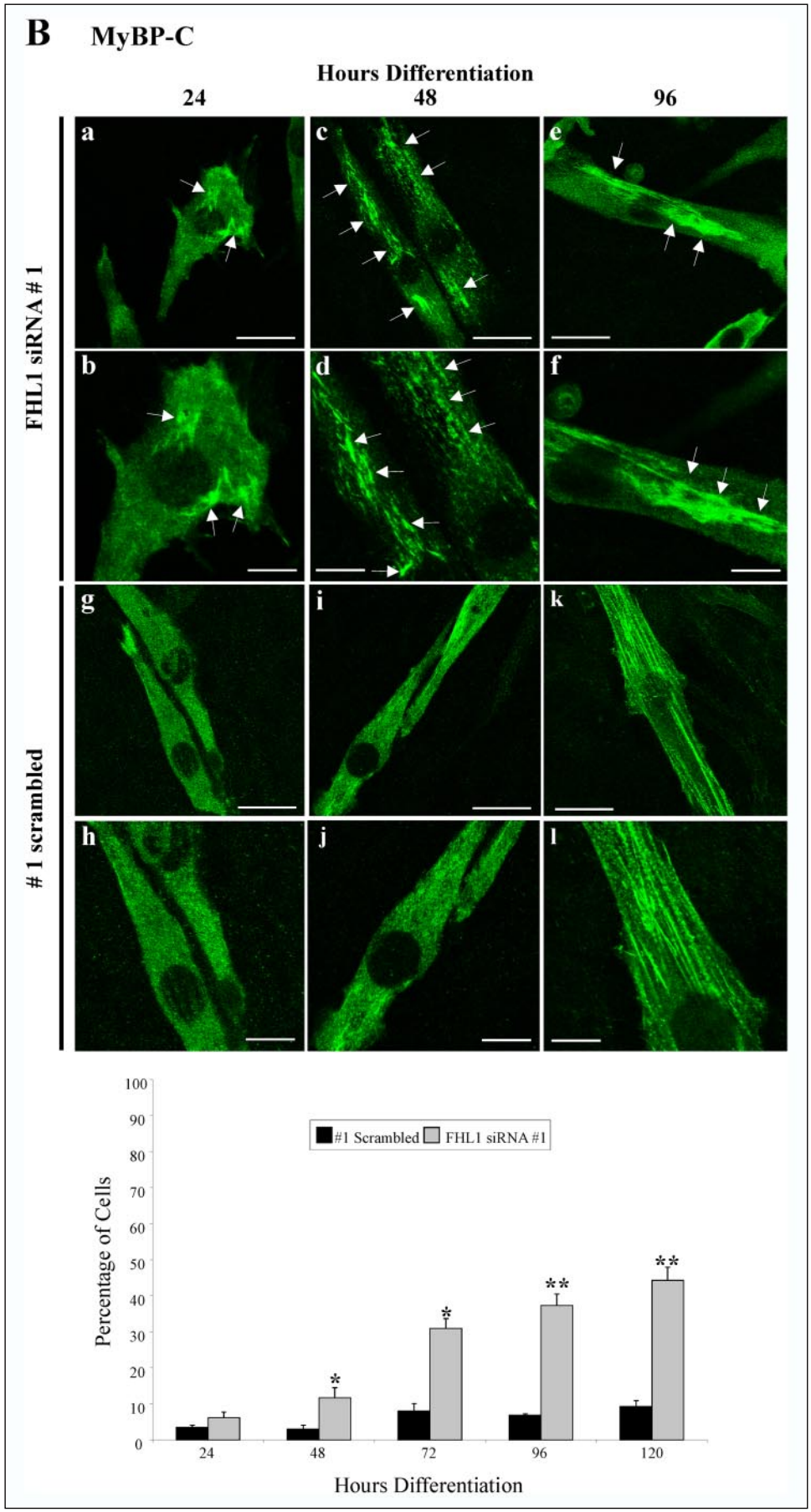

FIGURE 8—*continued*

comere formation, suggesting that binding of the C10 domain of MyBP-C to myosin may be critical for sarcomere formation (37, 38). As shown here overexpression of FHL1 in differentiating skeletal myoblasts resulted in myosac formation with impaired Z-line and myosin thick filament formation. Disruption of the sarcomere, particularly of thick filaments, has been associated previously with myosac formation. Inhibition of transglutaminase, which cross-links myosin thick filaments during myofibrillogenesis, leads to development of myosacs devoid of myofibrils (60). 12-*O*-Tetradecanoylphorbol acetate treatment of differentiating myoblasts results in disassembly of α-actin thin filaments and myosin thick filaments, and is associated with myosac formation (60, 61, 63, 64). In this regard disruption of the sarcomere is proposed to result in retraction of the growth tip of the myotube to form a sac-like myosac.

FHL1 RNAi-mediated knockdown was also associated with impaired thick filament formation and failure of MyBP-C to incorporate into the sarcomere. However, in contrast to overexpression studies, dense sheets of myosin and MyBP-C were detected in the cytosol. Previous studies have demonstrated that the effect of MyBP-C on myosin filament formation is dependent on the ratio of MyBP-C to myosin (26). Therefore, we predict that both overexpression and/or reduced FHL1 protein expression may alter the stoichiometry of the MyBP-C-myosin interaction. This may explain why both overexpression and underexpression of FHL1 were associated with the failure of myosin to assemble into thick filaments and impaired incorporation of MyBP-C into the sarcomere. We predict that during myofibrillogenesis, FHL1 regulates MyBP-C activity by inhibiting the interaction between MyBP-C and myosin.

The role of MyBP-C during sarcomere formation is contentious. In contrast to the effect of MyBP-C on myosin assembly in non-muscle COS-1 cells or isolated myocytes, *in vivo* studies indicate MyBP-C is important for thick filament stability but is not essential for thick filament cross-linking and sarcomere formation. For example, cardiac MyBP-C knock-out mice or transgenic mice expressing C-terminally truncated cardiac MyBP-C, lacking the C-terminal titin and/or myosin binding domains, develop a normal sarcomere that is only slightly misaligned (73–76). However, these *in vivo* studies were all performed in cardiac and not skeletal muscle, and it is the latter tissue in which FHL1 is most prominently expressed (77). Furthermore, FHL1 levels increase dramatically during skeletal muscle hypertrophy, induced by stretch or during periods of postnatal skeletal muscle growth, and therefore under these conditions excess FHL1 may effectively compete with skeletal myosin for MyBP-C (78, 79).

FHL1-induced Myosacs in Vitro May Correlate with Hypertrophy in Vivo—Experimental evidence from several unrelated studies indicates increased FHL1 mRNA levels strongly correlate with skeletal and cardiac muscle hypertrophy. FHL1 mRNA expression increases 10–15-fold during embryonic and postnatal skeletal muscle development (78). FHL1 mRNA levels also increase in stretch-induced skeletal muscle hypertrophy and decline during denervation-induced atrophy (79). However, it is not known if FHL1 itself triggers hypertrophy directly. Although this question cannot be answered directly by our study, it is noteworthy that emerging evidence suggests the development of myosacs *in vitro* may correlate with skeletal muscle hypertrophy *in vivo*. Expression of the cytokine interleukin-15 (IL-15) in differentiating murine C2 myoblasts induces myosac formation, and *in vivo*, IL-15 inhibits muscle wasting associated with cancer (cachexia) (66, 80). Insulin-like growth factor-1 (IGF-1) induces the formation of myosacs via calcineurin-mediated signaling, and IGF-1 transgenic mice develop pronounced skeletal hypertrophy, associated with persistent activation of calcineurin (62, 81, 82). Finally, inhibition of glycogen synthase kinase 3 (GSK-3) by phosphatidylinositol 3-kinase-PKB/Akt signaling contributes to IGF-1-mediated myosac formation in cultures of differentiating myoblasts, and expression of constitutively active Akt is sufficient to induce skeletal hypertrophy *in vivo* (68, 83–85).

FHL1 expression is also increased in hypertrophic human hearts (86–88). FHL1 expression is also increased in two mouse models of cardiac hypertrophy induced by aortic constriction and chronic β-adrenergic stimulation (89, 90). It is therefore intriguing that we have identified cardiac MyBP-C, mutations of which account for 20–30% of cases of familial hypertrophic cardiomyopathy, as an FHL1-binding partner (39). Most of these MyBP-C mutations result in truncation with loss of the C-terminal titin and/or myosin (C10) binding domains. Therefore, it is interesting to speculate that increased FHL1 and C-terminally truncated MyBP-C may both contribute, at least in part, to cardiac hypertrophy via a similar mechanism.

Acknowledgments—We thank Stephen Firth and Dr. Ian Harper (Monash MicroImaging, Monash University, Australia) for their assistance and technical advice regarding deconvolution microscopy. We also thank Dr. Lucie Carrier (INSERM U582, Institute de Myologie, Hospital Salpetriere, Paris, France) for generously providing the human cardiac MyBP-C cDNA.

REFERENCES

1. Louis, H. A., Pino, J. D., Schmeichel, K. L., Pomies, P., and Beckerle, M. C. (1997) *J. Biol. Chem.* **272,** 27484–27491
2. Flick, M., and Konieczny, S. (2000) *J. Cell Sci.* **113,** 1553–1564
3. Knoll, R., Hoshijima, M., Hoffman, H. M., Person, V., Lorenzen-Schmidt, I., Bang, M. L., Hayashi, T., Shiga, N., Yasukawa, H., Schaper, W., McKenna, W., Yokoyama, M., Schork, N. J., Omens, J. H., McCulloch, A. D., Kimura, A., Gregorio, C. C., Poller, W., Schaper, J., Schultheiss, H. P., and Chien, K. R. (2002) *Cell* **111,** 943–955
4. Arber, S., Hunter, J., Ross, J., Jr., Hongo, M., Sansig, G., Borg, J., Perriard, J., Chien, K., and Caroni, P. (1997) *Cell* **88,** 393–403
5. Mohapatra, B., Jimenez, S., Lin, J. H., Bowles, K. R., Coveler, K. J., Marx, J. G., Chrisco, M. A., Murphy, R. T., Lurie, P. R., Schwartz, R. J., Elliott, P. M., Vatta, M., McKenna, W., Towbin, J. A., and Bowles, N. E. (2003) *Mol. Genet. Metab.* **80,** 207–215
6. Pashmforoush, M., Pomies, P., Peterson, K. L., Kubalak, S., Ross, J., Jr., Hefti, A., Aebi, U., Beckerle, M. C., and Chien, K. R. (2001) *Nat. Med.* **7,** 591–597
7. Zhou, Q., Chu, P.-H., Cheng, C.-F., Martone, M. E., Knoll, G., Shelton, D. G., Evans, S., and Chen, J. (2001) *J. Cell Biol.* **155,** 605–612
8. Zhou, Q., Ruiz-Lozano, P., Martone, M. E., and Chen, J. (1999) *J. Biol. Chem.* **274,** 19807–19813
9. Bach, I. (2000) *Mech. Dev.* **91,** 5–17
10. Fimia, G. M., De Cesare, D., and Sassone-Corsi, P. (2000) *Mol. Cell. Biol.* **20,** 8613–8622
11. Morgan, M. J., and Madgwick, A. J. (1996) *Biochem. Biophys. Res. Commun.* **225,** 632–638
12. Yang, Y., Hou, H., Haller, E. M., Nicosia, S. V., and Bai, W. (2005) *EMBO J.* **25,** 1021–1032
13. McLoughlin, P., Ehler, E., Carlile, G., Licht, J. D., and Schafer, B. W. (2002) *J. Biol. Chem.* **277,** 37045–37053
14. Morlon, A., and Sassone-Corsi, P. (2003) *Proc. Natl. Acad. Sci. U. S. A.* **100,** 3977–3982
15. Yan, J., Zhu, J., Zhong, H., Lu, Q., Huang, C., and Ye, Q. (2003) *FEBS Lett.* **553,** 183–189
16. Martin, B., Schneider, R., Janetzky, S., Waibler, Z., Pandur, P., Kuhl, M., Behrens, J., von der Mark, K., Starzinski-Powitz, A., and Wixler, V. (2002) *J. Cell Biol.* **159,** 113–122
17. Du, X., Hublitz, P., Gunther, T., Wilhelm, D., Englert, C., and Schule, R. (2002) *Biochim. Biophys. Acta* **1577,** 93–101
18. Purcell, N., Darwis, D., Bueno, O., Muller, J., Schule, R., and Molkentin, J. (2004) *Mol. Cell. Biol.* **24,** 1081–1095
19. Wixler, V., Geerts, D., Laplantine, E., Westhoff, D., Smyth, N., Aumailley, M., Sonnenberg, A., and Paulsson, M. (2000) *J. Biol. Chem.* **275,** 33669–33678
20. Samson, T., Smyth, N., Janetzky, S., Wendler, O., Muller, J. M., Schule, R., von der Mark, H., von der Mark, K., and Wixler, V. (2004) *J. Biol. Chem.* **279,** 28641–28652
21. Coghill, I. D., Brown, S., Cottle, D. L., McGrath, M. J., Robinson, P. A., Nandurkar, H. H., Dyson, J. M., and Mitchell, C. A. (2003) *J. Biol. Chem.* **278,** 24139–24152
22. Winegrad, S. (1999) *Circ. Res.* **84,** 1117–11126
23. Weber, F. E., and Vaughan, K. T. (1993) *Eur. J. Biochem.* **216,** 661–669
24. Carrier, L., Bonne, G., Bahrend, E., Yu, B., Richard, P., Niel, F., Hainque, B., Cruaud, C., Gary, F., Labeit, S., Bouhour, J. B., Dubourg, O., Desnos, M., Hagege, A. A., Trent, R. J., Komajda, M., Fiszman, M., and Schwartz, K. (1997) *Circ. Res.* **80,** 427–434

25. Flashman, E., Redwood, C., Moolman-Smook, J., and Watkins, H. (2004) *Circ. Res.* **94,** 1279–1289
26. Craig, R., and Offer, G. (1976) *Proc. R. Soc. Lond. Ser. B Biol. Sci.* **192,** 451–461
27. Moos, C., Offer, G., Starr, R., and Bennett, P. (1975) *J. Mol. Biol.* **97,** 1–9
28. Okagaki, T., Weber, F. E., Fischman, D. A., Vaughan, K. T., Mikawa, T., and Reinach, F. C. (1993) *J. Cell Biol.* **123,** 619–626
29. Alyonycheva, T. N., Mikawa, T., Reinach, F. C., and Fischman, D. A. (1997) *J. Biol. Chem.* **272,** 20866–20872
30. Miyamoto, C. A., Fischman, D. A., and Reinach, F. C. (1999) *J. Muscle Res. Cell Motil.* **20,** 703–715
31. Gruen, M., and Gautel, M. (1999) *J. Mol. Biol.* **286,** 933–949
32. Starr, R., and Offer, G. (1978) *Biochem. J.* **171,** 813–816
33. Koretz, J. F. (1979) *Biophys. J.* **27,** 433–446
34. Sebillon, P., Bonne, G., Flavigny, J., Venin, S., Rouche, A., Fiszman, M., Vikstrom, K., Leinwand, L., Carrier, L., and Schwartz, K. (2001) *C. R. Acad. Sci. III* (*Paris*) **324,** 251–260
35. Seiler, S. H., Fischman, D. A., and Leinwand, L. A. (1996) *Mol. Biol. Cell* **7,** 113–127
36. Welikson, R. E., and Fischman, D. A. (2002) *J. Cell Sci.* **115,** 3517–3526
37. Gilbert, R., Kelly, M. G., Mikawa, T., and Fischman, D. A. (1996) *J. Cell Sci.* **109,** 101–111
38. Sato, N., Kawakami, T., Nakayama, A., Suzuki, H., Kasahara, H., and Obinata, T. (2003) *Mol. Biol. Cell* **14,** 3180–3191
39. Marian, A. J., and Roberts, R. (2001) *J. Mol. Cell. Cardiol.* **33,** 655–670
40. Watkins, H., Conner, D., Thierfelder, L., Jarcho, J. A., MacRae, C., McKenna, W. J., Maron, B. J., Seidman, J. G., and Seidman, C. E. (1995) *Nat. Genet.* **11,** 434–437
41. Brown, S., McGrath, M. J., Ooms, L. M., Gurung, R., Maimone, M., and Mitchell, C. A. (1999) *J. Biol. Chem.* **274,** 27083–27091
42. McGrath, M. J., Mitchell, C. A., Coghill, I. D., Robinson, P. A., and Brown, S. (2003) *Am. J. Physiol.* **285,** C1513–C1526
43. Robinson, P. A., Brown, S., McGrath, M. J., Coghill, I. D., Gurung, R., and Mitchell, C. A. (2003) *Am. J. Physiol.* **284,** C681–C695
44. Reinach, F., Masaki, T., Shafiq, S., Obinata, T., and Fischman, D. (1982) *J. Cell Biol.* **95,** 78–84
45. Knight, P. J., and Trinick, J. A. (1982) *Methods Enzymol.* **85,** 9–12
46. Lane, B., Elias, J., and Drummond, E. (1977) *J. Histochem. Cytochem.* **25,** 69–72
47. Pardo, J. V., Siliciano, J. D., and Craig, S. W. (1983) *Proc. Natl. Acad. Sci. U. S. A.* **80,** 1008–1012
48. Clarke, K. A., McElhinny, A. S., Beckerle, M. C., and Gregorio, C. C. (2002) *Annu. Rev. Cell Dev. Biol.* **18,** 637–706
49. Park, J. B., Kim, J. H., Kim, Y., Ha, S. H., Kim, J. H., Yoo, J. S., Du, G., Frohman, M. A., Suh, P. G., and Ryu, S. H. (2000) *J. Biol. Chem.* **275,** 21295–21301
50. Rybakova, I. N., Patel, J. R., and Ervasti, J. M. (2000) *J. Cell Biol.* **150,** 1209–1214
51. Berthier, C., and Blaineau, S. (1997) *Biol. Cell* **89,** 413–434
52. Dennis, J. E., Shimizu, T., Reinach, F. C., and Fischman, D. A. (1984) *J. Cell Biol.* **98,** 1514–1522
53. Bennett, P., Craig, R., Starr, R., and Offer, G. (1986) *J. Muscle Res. Cell Motil.* **7,** 550–567
54. Yang, Y. G., Obinata, T., and Shimada, Y. (2000) *Cell Struct. Funct.* **25,** 177–185
55. Littlefield, R., and Fowler, V. M. (2002) *Biophys. J.* **82,** 2548–2564
56. Starr, R., Almond, R., and Offer, G. (1985) *J. Muscle Res. Cell Motil.* **6,** 227–256
57. Morgan, M., and Madgwick, A. (1999) *Biochem. Biophys. Res. Commun.* **255,** 245–250
58. Kong, Y., Flick, M. J., Kudla, A. J., and Konieczny, S. F. (1997) *Mol. Cell. Biol.* **17,** 4750–4760
59. Saitoh, O., Arai, T., and Obinata, T. (1988) *Cell Tissue Res.* **252,** 263–273
60. Kang, S. J., Shin, K. S., Song, W. K., Ha, D. B., Chung, C. H., and Kang, M. S. (1995) *J. Cell Biol.* **130,** 1127–1136
61. Mermelstein Cdos, S., Costa, M. L., Chagas Filho, C., and Moura Neto, V. (1996) *J. Muscle Res. Cell Motil.* **17,** 199–206
62. Musaro, A., McCullagh, K. J. A., Naya, F. J., Olson, E. N., and Rosenthal, N. (1999) *Nature* **400,** 581–585
63. Lin, Z. X., Eshelman, J. R., Forry-Schaudies, S., Duran, S., Lessard, J. L., and Holtzer, H. (1987) *J. Cell Biol.* **105,** 1365–1376
64. Lin, Z. X., Eshleman, J., Grund, C., Fischman, D. A., Masaki, T., Franke, W. W., and Holtzer, H. (1989) *J. Cell Biol.* **108,** 1079–1091
65. Quinn, L. S., Haugk, K. L., and Grabstein, K. H. (1995) *Endocrinology* **136,** 3669–3672
66. Quinn, L. S., Anderson, B. E., Drivdahl, R. H., Alvarez, B., and Argiles, J. M. (2002) *Exp. Cell Res.* **280,** 55–63
67. Palmer, S., Groves, N., Schindeler, A., Yeoh, T., Biben, C., Wang, C.-C., Sparrow, D. B., Barnett, L., Jenkins, N. A., Copeland, N. G., Koentgen, F., Mohun, T., and Harvey, R. P. (2001) *J. Cell Biol.* **153,** 985–997
68. Rochat, A., Fernandez, A., Vandromme, M., Moles, J. P., Bouschet, T., Carnac, G., and Lamb, N. J. (2004) *Mol. Biol. Cell* **15,** 4544–4555
69. Bader, D., Masaki, T., and Fischman, D. (1982) *J. Cell Biol.* **95,** 763–770
70. Lange, S., Auerbach, D., McLoughlin, P., Perriard, E., Schafer, B. W., Perriard, J. C., and Ehler, E. (2002) *J. Cell Sci.* **115,** 4925–4936
71. Ervasti, J. M. (2003) *J. Biol. Chem.* **278,** 13591–13594
72. Mayer, U., Saher, G., Fassler, R., Bornemann, A., Echtermeyer, F., von der Mark, H., Miosge, N., Poschl, E., and von der Mark, K. (1997) *Nat. Genet.* **17,** 318–323
73. Yang, Q., Sanbe, A., Osinska, H., Hewett, T. E., Klevitsky, R., and Robbins, J. (1998) *J. Clin. Investig.* **102,** 1292–1300
74. Yang, Q., Sanbe, A., Osinska, H., Hewett, T. E., Klevitsky, R., and Robbins, J. (1999) *Circ. Res.* **85,** 841–847
75. Harris, S. P., Bartley, C. R., Hacker, T. A., McDonald, K. S., Douglas, P. S., Greaser, M. L., Powers, P. A., and Moss, R. L. (2002) *Circ. Res.* **90,** 595–601
76. Carrier, L., Knoll, R., Vignier, N., Keller, D. I., Bausero, P., Prudhon, B., Isnard, R., Ambroisine, M. L., Fiszman, M., Ross, J. J., Schwartz, K., and Chien, K. R. (2004) *Cardiovasc. Res.* **63,** 293–304
77. Brown, S., Biben, C., Ooms, L. M., Maimone, M., McGrath, M. J., Gurung, R., Harvey, R. P., and Mitchell, C. A. (1999) *J. Mol. Cell. Cardiol.* **31,** 837–843
78. Morgan, M. J., Madgwick, A., Charleston, B., Pell, J. M., and Loughna, P. T. (1995) *Biochem. Biophys. Res. Commun.* **212,** 840–846
79. Loughna, P. T., Mason, P., Bayol, S., and Brownson, C. (2000) *Mol. Cell Biol. Res. Commun.* **3,** 136–140
80. Carbo, N., Lopez-Soriano, J., Costelli, P., Busquets, S., Alvarez, B., Baccino, F. M., Quinn, L. S., Lopez-Soriano, F. J., and Argiles, J. M. (2000) *Br. J. Cancer* **83,** 526–531
81. Musaro, A., McCullagh, K., Paul, A., Houghton, L., Dobrowolny, G., Molinaro, M., Barton, E., Sweeney, H., and Rosenthal, N. (2001) *Nat. Genet.* **27,** 195–200
82. Musaro, A., and Rosenthal, N. (1999) *Mol. Cell. Biol.* **19,** 3115–3124
83. Rommel, C., Bodine, S. C., Clarke, B. A., Rossman, R., Nunez, L., Stitt, T. N., Yancopoulos, G. D., and Glass, D. J. (2001) *Nat. Cell Biol.* **3,** 1009–1013
84. Vyas, D. R., Spangenburg, E. E., Abraha, T. W., Childs, T. E., and Booth, F. W. (2002) *Am. J. Physiol.* **283,** C545–C551
85. Bodine, S. C., Stitt, T. N., Gonzalez, M., Kline, W. O., Stover, G. L., Bauerlein, R., Zlotchenko, E., Scrimgeour, A., Lawrence, J. C., Glass, D. J., and Yancopoulos, G. D. (2001) *Nat. Cell Biol.* **3,** 1014–1019
86. Hwang, D. M., Dempsey, A. A, Wang, R. X., Rezvani, M., Barrans, J. D., Dai,K. S., Wang, H. Y., Ma, H., Cukerman, E., Liu, Y. Q., Gu, J. R., Zhang, J. H.,Tsui, S. K., Waye, M. M. Y., Fung, K. P., Lee, C. Y., and Liew, C. C. (1997) *Circulation* **96,** 4146–4203
87. Hwang, D. M., Dempsey, A. A., Lee, C. Y., and Liew, C. C. (2000) *Genomics* **66,** 1–14
88. Lim, D. S, Roberts, R., and Marian, A. J. (2001*) J. Am. Coll. Cardiol.* **38,** 1175–118
89. Chu, P. H., Ruiz-Lozano, P., Zhou, Q., Cai, C., and Chen, J. (2000) *Mech.Dev.* **95,** 259–265
90. Gaussin, V., Tomlinson, J. E., Depre, C., Engelhardt, S., Antos, C. L.,Takagi, G., Hein, L., Topper, J. N., Liggett, S. B., Olson, E. N., Lohse, M.J., Vatner, S. F., and Vatner, D. E. (2003) *Circulation* **108,** 2926–2933
91. Thompson, J. D., Higgins, D. G., and Gibson, T. J. (1994) *Nucleic Acids Res.* **22,** 4673–4680